Master's Thesis

Investigating adhesion and stretchability of acrylate-based pressure sensitive adhesives

Ju Hak Lee

Department of Chemical Engineering

Graduate School of UNIST

2020

Investigating adhesion and stretchability of acrylate-based pressure sensitive adhesives

Ju Hak Lee

Department of Chemical Engineering

Graduate School of UNIST

Investigating adhesion and stretchability of acrylate-based pressure sensitive adhesives

A thesis/dissertation
submitted to the Graduate School of UNIST
in partial fulfillment of the
requirements for the degree of
Master of Science

Ju Hak Lee

11. 26. 2019
Approved by

Advisor
Dong Woog Lee

Investigating adhesion and stretchability of acrylate-based pressure sensitive adhesives

Ju Hak Lee

This certifies that the thesis/dissertation of Ju Hak Lee is approved.

11. 26. 2019

signature

Advisor: Dong Woog Lee

signature

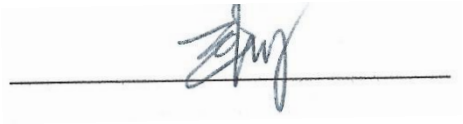

Hak-Sun Kim

signature

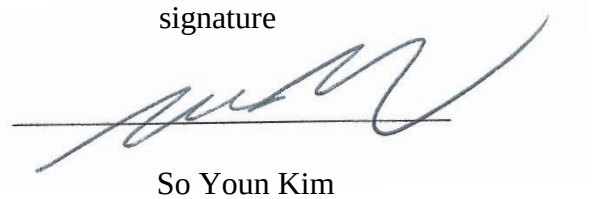

So Youn Kim

Abstract

Soft adhesives have been emerged as pertinent materials for display assembly motivated by the high demand of stretchable/flexible display employed for not only everyday use electronics such as mobile phones or smart watches but also specialized devices such as epidermal electronics for health monitoring system. This thesis explored fundamental works to develop stretchable/flexible pressure sensitive adhesives (PSAs) in terms of effect of monomer functionalities (e.g., $-CH_3$, $-NH_2$, -OH and -COOH) and compositional effect of acrylic acid, focusing on the reciprocal relation between their stretchability and adhesion as well as their optimization. Adhesion performance of the PSAs was estimated in accordance with ASTM D3330 using 180° peel adhesion test. Repetitive cycle test was implemented to directly estimate strain reversibility of the PSAs under sequential mechanical stress. Eligibility of the PSAs for the device application was evaluated via light transmittance (%T) and metal-corrosiveness test using a corrosion-sensitive layer (Indium Tin Oxide). Apart from the practical investigation of the PSAs for the display application, adhesion mechanism of acrylic acid-incorporated PSAs was systematically explored, which have been remained as an unresolved issue with debates. This research, as a fundamental study of innovative PSAs, will endow chemical and industrial engineers with design guidelines for new types of PSAs with advanced properties compatible with contemporary devices.

Blank page

Contents

List of Figures

List of Tables

Chapter 1. Introduction

Along the developments of advanced devices in industries (e.g., aircraft, automobile and electronics), the demand for pertinent materials has been steeply increasing. For instance, an advent of contemporary devices such as the Internet of Things emphasizes an importance of human-machine interface achieved through displays acting as vital components[1, 2]. This is because displays exhibit data from machines to users and feedback can be granted to machines through the users' response[2]. Displays have been developed from the stiff plane shape (e.g., SAMSUNG Galaxy S1 and Apple iPhone 1) to having flexibility or curvature (e.g., SAMSUNG Galaxy S9 Plus and Nubia Alpha Smart watches) to increase intimacy of electronics with users. Not only are flexible and stretchable displays applied in everyday use electronics such as mobile phones and smart watches for user convenience, but also these features are indispensable for specialized devices such as epidermal electronics with advanced bioinspired designs for health care systems[3, 4].

Conventionally, optically clear adhesives (OCAs) and optically clear resins (OCRs) have been widely employed to assemble display components. However, these are no longer suitable for the contemporary devices demanding stretchability/flexibility due to their unrestorable conformation upon stretching or folding and large stiffness[5, 6].

Pressure sensitive adhesives (PSAs) which are subordinate to OCAs have been emerging as prospective candidates for stretchable/flexible adhesives thanks to their advantages compared to OCRs (e.g., intrinsic flexibility, high viscoelasticity and minimizing the refractive index discrepancy) [7-9]. In addition, absence of post-treatments such as solvent evaporation and setting through heat or chemical reaction make PSAs distinguishable over all other classes of adhesives[10]. There are three types of commonly used PSAs (e.g., acrylate-, rubber- and silicone-based). Among these, acrylic PSAs are widely used in various industrial fields because of a large variety of monomers with different functionalities which enable manifold material designs[11].

Acrylic PSAs are composed of three major segments; soft (low T_g), hard (high T_g) and functional monomers[12]. The soft monomers are necessary for a tacky material which is related to wetting. The hard monomers are employed to give internal strength. And the functional monomers such as acrylic acid and acrylamide are implemented into the monomer mixture for incorporation of adhesive sites[13].

Acrylate-based PSAs can be prepared through thermal or photo-induced polymerization relying on the method of the initiation. The use of solvent, energy costs, time consumption in the thermal

processing and constraints imposed by environmental pollution regulations have led to the development of more user and environmental friendly processing[14]. The benefits of the UV-curing systems, including lower process costs, solvent-free and rapid production rate in a small place[15], have contributed to its wide use in industries.

However, mere acrylic monomer solution has poor workability for UV-curing system due to its liquidity as it is casted onto a releasing film prior to UV-curing. To resolve this issue, fillers have been incorporated to control initial viscosity of the mixture[16]. There are various types of fillers for adhesives, and fumed silica has been one of the most frequently used fillers for acrylate-based adhesives[17]. The degree of compatibility with the employed acrylic monomers can be enhanced depending on hydrophobicity of fumed silica based on 'like dissolves like' rule.

Although the mechanical properties (e.g., peel, tack and shear) of PSAs have been studied in detail for last decades[18, 19], physical properties of acrylate-based PSAs related to stretchable/flexible adhesives are not systematically investigated as a function of monomer types and compositions. Plus, adhesion mechanism of acrylic acid-incorporated PSAs is not fully understood despite its outstanding adhesion performance[20].

The thesis focuses on systematic characterization of physical properties of acrylate-based UV-curable PSAs with respect to incorporation of various acrylic monomers (Chapter 2), and adhesion mechanism of acrylic acid-incorporated PSAs showing the excellent peel adhesion (Chapter 3). Additionally, the investigation of the compositional effect of fabricated PSAs with acrylic acid content uncovered a measures to achieve instantaneous strain reversibility as well as to tailor physical properties of the PSAs (Chapter 4). The overall findings are expected to give rise to positive contribution to the development of advanced PSAs for a wide range of contemporary device application.

Chapter 2. Effect of acrylic monomer functionalities

2.1 Experimental method and materials

2.1.1 Preparation of UV curable PSAs

Acrylic PSAs were prepared by using various acrylic monomers through UV curing. Acrylic monomers containing different functional groups; methyl acrylate (MA, Sigma-Aldrich, USA), acrylic acid (AA, Sigma-Aldrich, USA), acrylamide (AM, Alfa Aesar, USA), and 2-hydroxyethyl acrylate (HEA, TCI Chemicals, Japan) were mixed (30 mol%) to 70 mol% of the base monomer (2-Ethylhexyl acrylate, EHA, Sigma-Aldrich, USA). Each functional monomer contains one functional group, which makes the content of functional groups to 30 mol% in each PSA. Based on the typical composition[13], this mixing ratio was chosen to investigate the monomers' individual effect on the physical properties of the synthesized PSAs. The overall chemical composition is summarized in Table 2.1 and each random copolymer formula is shown in Figure 2.1 a-d. Each chemical mixture was prepared using vortex mixer after addition of 15 wt% of hydrophobic fumed silica (Aerosil R 972, Evonik Industries, Germany) as a filler and 0.3 wt% (2 wt% of the fumed silica) of the dispersing agent (DISPERBYX 2158, BYK, Germany) into the solution mixture. Hexanediol diacrylate (HDDA, Alfa Aesar, USA) was used as a crosslinking agent. Phenylbis (2,4,6-trimethyl-benzoyl) phosphine oxide (TCI Chemicals, Japan) was used as a photoinitiator. The mixture was coated on the releasing film (SG31, SKC, South Korea) using

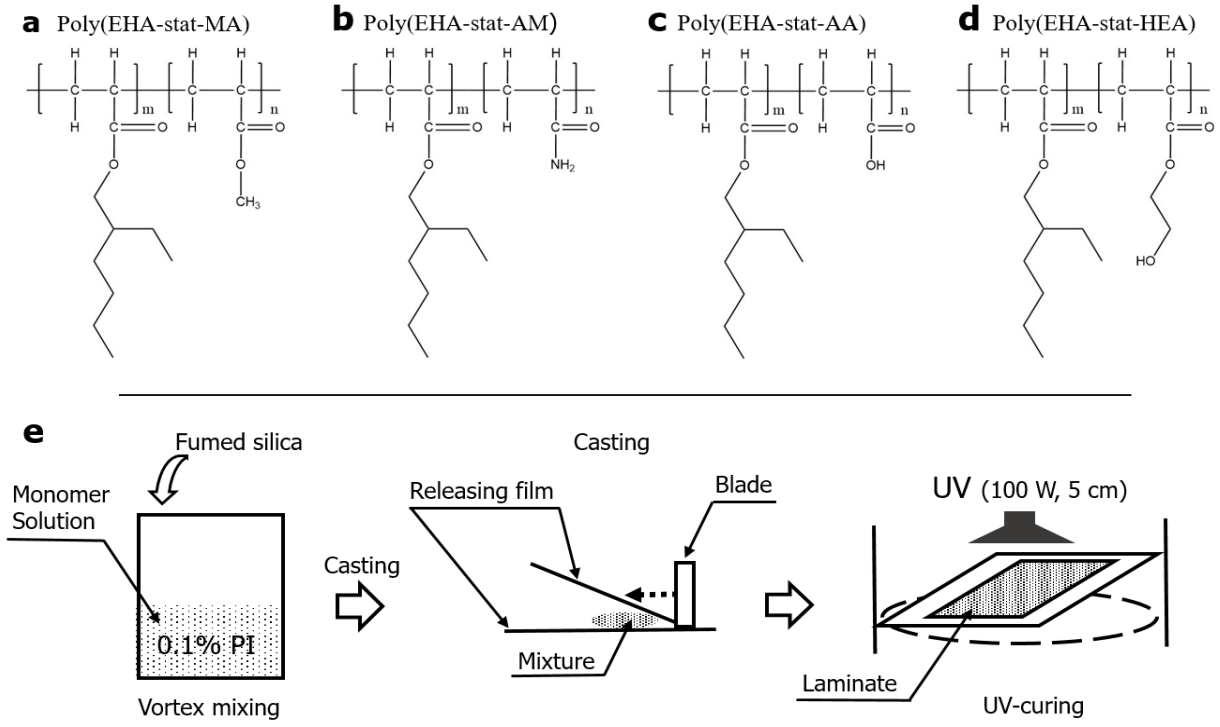

Figure 2.1 Random copolymer formulas with various acrylic monomers (a) poly(EHA-stat-MA), (b) poly(EHA-stat-AM), (c) poly(EHA-stat-AA), (d) poly(EHA-stat-HEA) and (e) schematic diagrams of UV curable PSAs fabrication process.

the knife coating device (KP-3000VH, KIPAE, South Korea), finally prepared into a laminated form. The laminate was cured under the UV lamp (100W, 365 nm) with a certain curing time and distance of 5 cm. The synthesis process of UV curable PSAs is illustrated in Figure 2.1 (e). Note that 1.5 ml of ethanol was used as a solvent to dissolve acrylamide monomer. The synthesized PSAs had thickness (B) of 100±10 μm. Thicker PSA specimens for the repetitive cycle test were chosen (B is 230±15μm for better handling. All of the PSAs showed optically clear appearance except 3AM. A molecular weight measurement was inaccessible because all of the synthesized PSAs were insoluble in common organic solvents such as tetrahydrofuran and ethyl acetate due to the crosslinking.

Table 2.1 Chemical composition of acrylic monomers used to prepare PSAs. Each number signifies mol percent. All samples include HDDA (0.25 mol%) and PI (0.1 mol%), fumed silica (15 wt%), and dispersing agent (0.3 wt%), with respect to total monomer concentration and weight.

Chemicals	EHA	MA	AA	AM	HEA
3MA	70	30			
3AA	70		30		
3AM	70			30	
3HEA	70				30

2.1.2 Peel adhesion test

Peel adhesion specimens were prepared with the dimensions of 25 mm x 300 mm (W x L), followed by pressing on the SUS (stainless steel) panel by 2.5 kg roller twice in lengthwise direction. The peel adhesion test was conducted at the crosshead speed of 300 mm/min after 15 min of dwell time at room temperature using the universal testing machine (WL2100C, Withlab, South Korea). The peel adhesion was calculated according to ASTM D3330, Test Method A., and the given values are the average of at least 3-repetition.

2.1.3 Repetitive cycle test

100-repetitive cycle test was performed with the specimen dimensions of 13 mm x 38 mm (W x L) using a tensile strength measurement (DAO-u01, DAO Technology, South Korea) at room temperature. Each specimen was subjected to 15% strain, with the crosshead speed of 500 mm/min. Hysteresis loss of each specimen was obtained by numerical integration of the area between elongation and contraction curves of the stress-strain curves[21].

2.1.4 Rheological properties measurement

Rheological properties were measured using a rheometer (Kinexus pro+, Malvern Panalytical Ltd, UK). Oscillation frequency was varied from 0.01 to 100 Hz at 0.025% of strain and the specimens were subjected to the temperature of 25°C[22]. The gap between the zig and the bottom plate was adjusted in order to achieve the force range of ~0.2 N-0.3 N.

2.1.5 Transmittance measurement

Double beam spectrometer was used to measure the transmittance of the synthesized UV curable PSAs using UV-Vis-NIR spectroscopy (Cary 5000, Varian, USA). PSA-attached glass and bare glass were used as the specimen and reference material, respectively. The scanned wavelength range to determine the transmittance was 300-700 nm.

2.2 Results and discussion

2.2.1 Peel adhesion test

When a PSA is peeled, the pulling force is transferred from a backing material to the substrate-adhesive interface of the peel front (three-phase contact line of the adhesive, the substrate and air where peeling occurs). This force causes the PSA to be peeled off from the substrate, while the peel front is migrated to the opposite side where peeling occurs until the PSA is completely peeled off. Since the backing material and the SUS panel are sufficiently stiff to avoid deformation, the energy must be dissipated as heat through stretching and relaxation motion of the adhesive[23]. The energy absorbed or dissipated per unit area of the interface peeled is regarded as peel adhesion. This energy is determined by both the

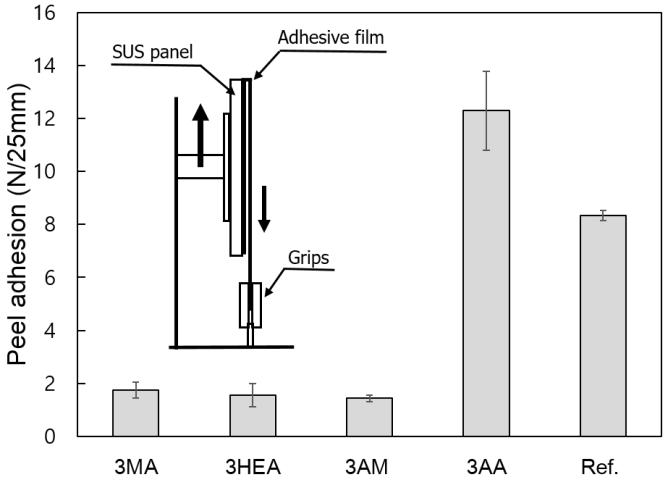

Figure 2.2 Peel adhesion of the synthesized PSAs with various acrylic monomers. Ref. represents 'Scotch tape' (PK65 48x40 Transparent, 3M, USA).

interfacial forces of the adhesives and the ability of the adhesives to dissipate energy in the bulk. Figure 2.2 shows the peel adhesion values of acrylic monomer incorporated PSAs. AA incorporated PSAs exhibited the highest peel adhesion (12.3 ± 1.2 N/25 mm) while MA, HEA and AM added PSAs showed relatively low adhesion with no significant difference one another (~2 N/25mm). Generally accepted debonding mechanism is cavity-fibril formation which indicates the creation of cavities and fibril stretching, and it depends on the functional groups of the copolymers[20]. Hydrogen bonds along with the acid moieties can increase cohesion, meaning that it takes more energy to break the bonds and elongate the polymer chains. Thus, the amount of energy necessary to stretch the fibrils increases, resulting in high peel adhesion. AM added PSAs should have exhibited comparable peel adhesion to that of AA incorporated PSAs, due to its amine groups which can also act as a hydrogen bonding site. Yet, silica aggregation and phase separation indicated by opaque appearance may have caused negative contributions to the expected interfacial forces as well as energy absorption, leading to the lowest peel adhesion. 3MA represented slightly higher peel adhesion than 3HEA which reflects that the effect of hydroxyl groups is practically negligible despite its capability of hydrogen bonding, leading to the low energy dissipation in peeling process as poor as 3MA. Only 3AA has displayed significantly high peel adhesion (12.3 ± 1.2 N/25mm), which was even higher than the peel adhesion (8.34 ± 0.2 N/25mm) of commonly used 'Scotch tape' (PK65 48x40 Transparent, 3M, USA).

2.2.2 Repetitive cycle test

The adhesives for stretchable display applications must show elastomeric performance, meaning that these must be able to have rapid strain reversibility after elongation. Since amorphous polymers exist in a random coil structure, the molecules will uncoil to the limited linear structure as elongated[24]. In thermodynamic point of view, the entropy of an elastomer is decreased as the elastomer is strained to the linear conformations, while the entropy is increased as an elastomer is returned to the original random coil structure due to the numerous possible conformations of macromolecules. Thus, strain reversibility is thermodynamically favored phenomenon in case of amorphous polymers. And in order to obtain rapid strain reversibility**,** the formation of new intermolecular bonds (e.g., hydrogen bonds) after stretching should be minimized, and bulky pendant groups which can limit the recoiling process should be avoided as much as possible. Furthermore, crosslinking is an indispensable component to prevent relative translational motion during straining, which can provide percolation network throughout the bulk, resulting in strain reversibility[24]. This is the reason for using 0.25 mol% of HDDA, which was mixed into the solution mixture before curing. Figure 2.3 shows the 100-cycle stress-strain curves of acrylate based PSAs. All of four types of PSAs display Mullins effect which indicates the disentanglement of chains occurred at the first strain, and thus the stress required for subsequent cycles is decreased. Hysteresis loss (HL) is defined as the area between loading and unloading curves

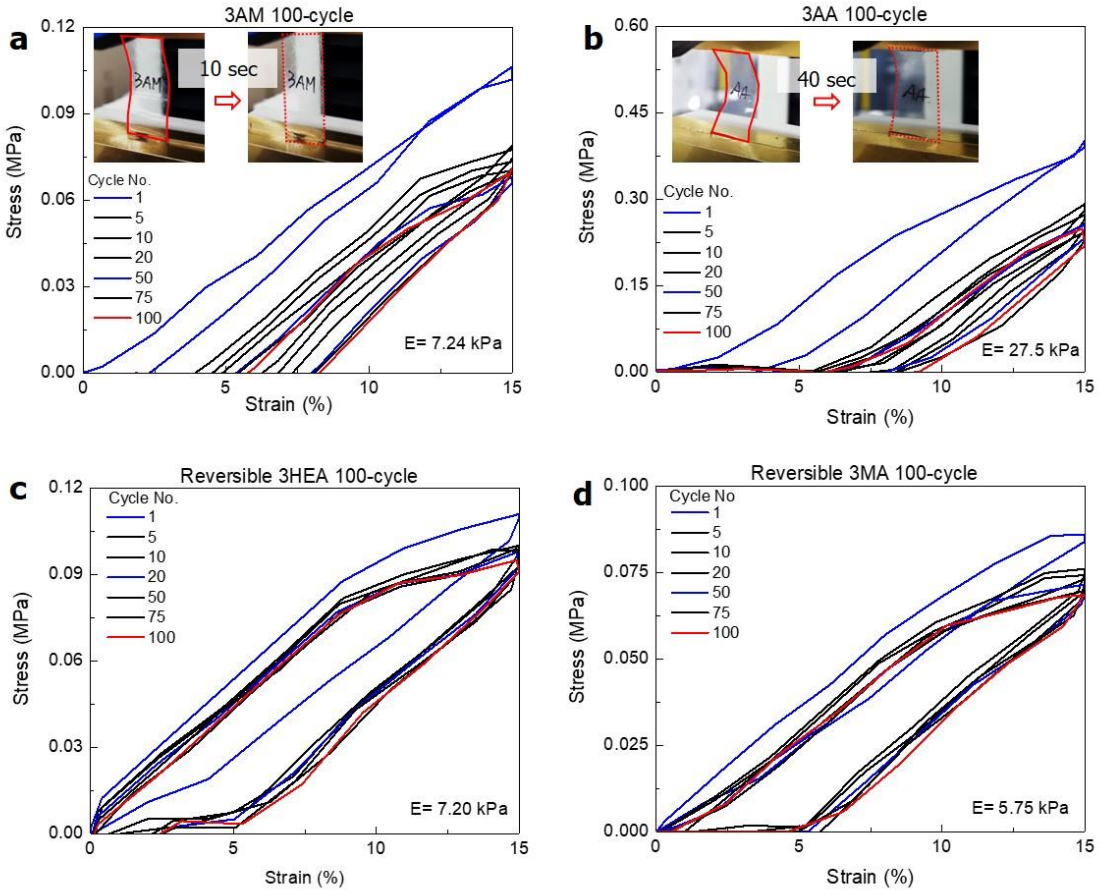

Figure 2.3 The 100-cycle stress-strain curves of acrylate-based PSAs with various acrylic monomers (a) AM, (b) AA, (c) HEA, and (d) MA.

representing the energy lost during each cycle. The HL values of each PSA are plotted in Figure 2.4 as a function of number of cycles. The HL of 3AA increases with subsequent cycles, which indicates that more energy is lost with increasing number of cycles. It suggests that entanglements of those polymers can be removed with repeated loading/unloading cycles, thereby dissipating more energy as heat. However, rest of PSAs exhibited relatively constant HL as subjected to subsequent stress. 3AM and 3AA have displayed slow and partial recovery after 100-cycle test, respectively, while 3MA and 3HEA PSAs have exhibited instantaneous strain reversibility (Figure 2.3). The reason for 3AA having partial recovery is that acrylic acid is able to provide hydrogen bonds, which are strong physical bonds that can break and reform during the loading and the unloading, restraining reversibility of extended polymer chains to their zero strain. Accordingly, the 3AA exhibits increasing HL (Figure 2.4 a) with increasing number of cycles and long recovery time (40 sec) with the failure of the full restoration after 100 cycles. The lowest HL of 3AM throughout the cycles suggests the incorporation of acrylamide with the solvent causes imperfect synthesis of the PSA since the effect of hydrogen bonds does not exist in spite of its availability. It coincides with relatively short recovery time (10 sec) with full recovery after 100 cycles. It is worthy noted that hydroxyl groups of 3HEA do not participate in hindrance of

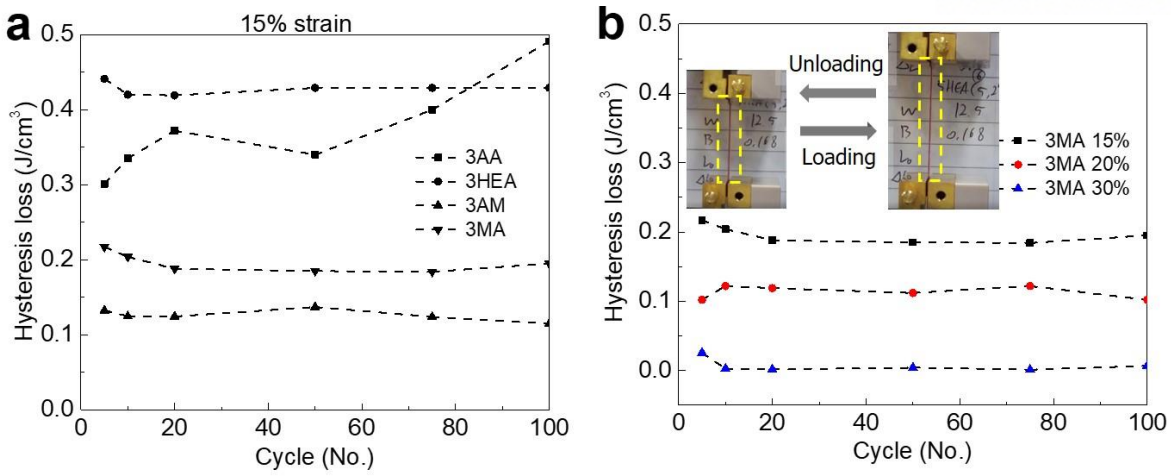

Figure 2.4 The plot of hysteresis loss change of each specimen for 100-cycle test with fixed 15% strain (a). The plot of hysteresis loss change of 3MA w. r. t. different strains during 100-cycle test (b). The hysteresis loss of the first cycle is excluded.

reversibility, rather than provide instantaneous reversibility. This suggests that the effect of hydrogen bonds formed by hydroxyl groups on the reversibility is minor, which also doesn't seem to contribute to the peel adhesion. However, this effect becomes obvious as stiffness (or Young's modulus, E) of PSAs is concerned (Figure 2.3). Methyl groups in 3MA offer weak van der Waals force along polymer chains which is not strong enough to disturb chain recoiling, resulting in prompt strain reversibility. The results suggest that steady HL is of importance to obtain instantaneous strain reversibility. 3MA, which exhibited minimum HL and instantaneous strain reversibility, was subjected to the repetitive cycle with larger strain (20% and 30%). The results (Figure 2.4 b) exhibited a decrease of HL as strain increases, meaning that its elastic performance is enhanced at higher strain. According to the thermodynamics of the rubber elasticity, restoring force depends only on the rate of change of entropy with length[25]. At higher strain, there is more number of fully extended length of a chain segment, whereas the major segments remain as random-coil state at lower strain. This difference gives rise to the change in entropy. A large entropic change is achieved at a high strain, resulting in high entropic restoring force. Hence, the elastic performance of 3MA can be enhanced at higher strain.

2.2.3 Rheological properties

Due to viscoelastic behavior of PSAs, they behave as soft solids (e.g., silly putty) than as liquids (e.g., water) during wetting process. PSAs are soft enough to deform sufficiently to form intimate contact with the substrate, but they keep some elastic memory at least for a time after bond formation. Thus, the modulus is the main factor which dictates the resistance to the wetting flow, i.e. lower modulus, better wetting. In order to provide intimate wetting, interfacial properties of a material must overcome the resistance to the flow, which is determined by its modulus. It is generally reported that the storage modulus (G') at 1 Hz is related to wetting of PSAs[22]. The lower G' indicates less resistance to the flow,

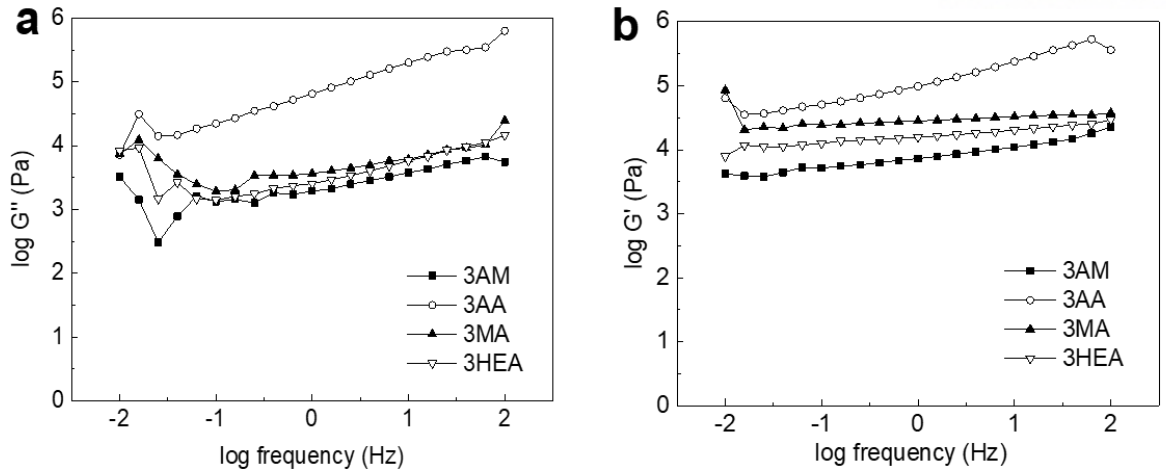

Figure 2.5 Rheological properties of the synthesized PSAs with various acrylic monomer types; (a) loss modulus and (b) storage modulus.

resulting in larger wetting area. However, the storage modulus does not contain any information about the PSA's ability to resist debonding (i.e., adhesion energy). In order for PSAs to absorb more energy, they should be able to effectively dissipate energy through molecular motions. Loss modulus (G") at 100 Hz is normally used to depict how much energy can be lost during debonding process, relating to peel adhesion[22]. The order of loss modulus at 100 Hz of each PSA shown in Figure 2.5 corresponds to the order of their peel adhesion, which means 3AA is able to dissipate the most energy among others. One may concern the influence of acid groups on the surface exerting peel adhesion. Falsafi et al. measured the surface energies of crosslinked 2-ethylhexyl acrylate-co-acrylic acid elastomers, which were approximately 30 mJ m^{-2}, indicating that the surfaces are dominated by methylene groups[26]. They hypothesized that the carboxyl groups of the polymer prefer to stay in the bulk of the PSAs and supported this hypothesis by analyzing XPS data showing that carbon enrichment over in the vicinity of the surface. Accordingly, the effect of surface functionality on peel adhesion is expected to be negligible. Peel adhesion of lightly crosslinked PSAs is dependent on how much energy can be dissipated during peeling process. 3AA showed highest peel adhesion despite its highest G' at 1 Hz, indicating poor wetting as compared to others. The possible explanation is that its high resistance to deformation could be overwhelmed by its ability to dissipate energy so that overall combined effect of the moduli puts 3AA first over other PSAs in terms of peel adhesion.

2.2.4 Optical properties and evaluation

Figure 2.6 shows the transmittance (%T) measurement of PSAs. The synthesized PSAs exhibit excellent transmittance (95 %T) in both visible and UV ranges except 3AM. The fabricated 3AM PSAs were optically opaque and silica aggregation with phase separation was observed (Figure 2.7 a). Needle-like crystals were observed on the surface of the 3AM mixture during the laminate-formation processing, which is caused by the favorable solvent evaporation. Yet, it does not guarantee that every single solvent

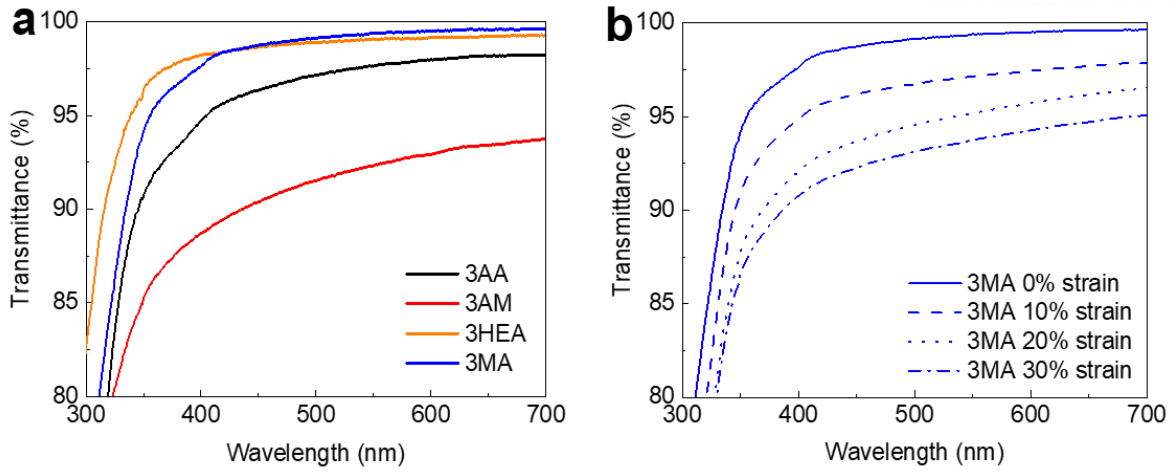

Figure 2.6 Transmittance measurement (%T) of the (a) synthesized PSAs at zero strain, and (b) 3MA strained up to ~30%.

molecule is removed clearly due to the fast processing rate (~ 4 min). The colorless solvent turned the cloudy as the filler was added and it became a grease-like fluid as the amount of the filler increases. It signifies the solvent plays a role to aggregate the filler particles, leading to the phase separation. Thus, the remaining solvent may give rise to the particle aggregation with the separation from the polymer matrix, resulting in the optically opaque of the 3AM. In a display point of view, since high transmittance in blue range reduces yellow index, these PSAs can be used without constraining the transparency of the assembled display. Since 3MA showed instantaneous strain reversibility with the lowest and constant hysteresis loss, its %T was measured while straining (Figure 2.6 b). The decrease of %T was measured as increasing strain, which might be due to the increase in crystallinity of the structure or breakdown of silica network, re-alignment or orientation of the filler[27, 28]. The %T is recovered after the removal of stress, which is another indication that 3MA is fully restorable. 3MA was further subjected to evaluation test (Figure 2.7) to prove its optical clarity for the display purpose as strained. The letters were written ‘on’ the PSA (Figure 2.7 c-e) to check their sustainability. In addition, the visual transparency through the PSA was tested (Figure 2.7 f-g) by observing letters ‘below’ the PSA. The results demonstrate its feasibility of use as a stretchable adhesive for the stretchable display application.

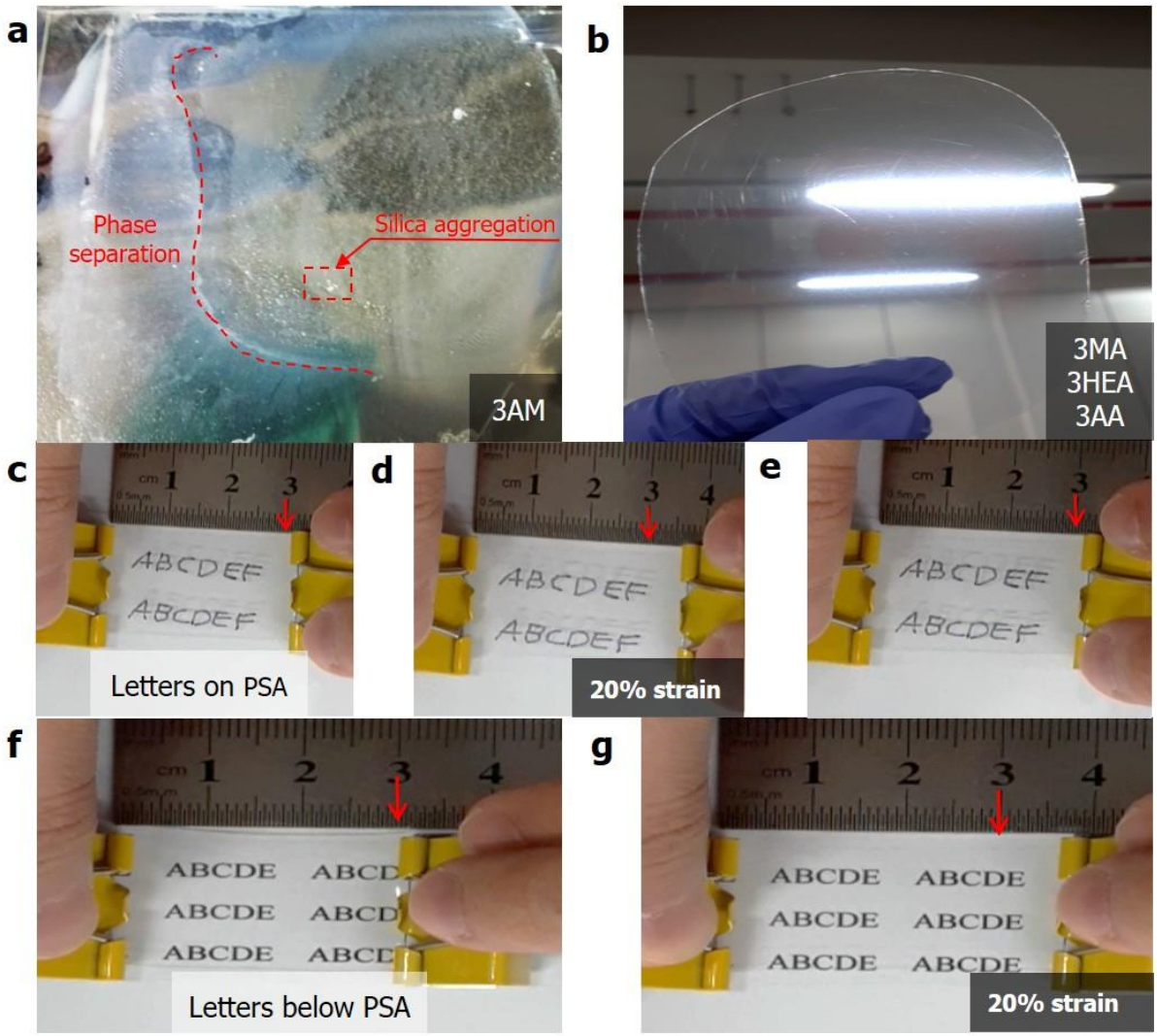

Figure 2.7 (a) 3AM PSA, (b) and other PSAs after curing. (c, d, e) figures of 3MA PSA showing letters on the PSA before and after stretching (20% strain). (f, g) Figures of 3MA PSA showing letters below the PSA before and after stretching (20% strain).

2.3 Conclusions

Acrylate-based PSAs were synthesized using UV curing method, and their physical properties with respect to various acrylic monomers were successfully characterized. In this characterization, AA incorporation showed the highest peel adhesion among others and this result coincides with the trend of the loss modulus values. Instantaneous strain reversibility was achieved through the formulation using MA and HEA. 3MA proved its instantaneous strain reversibility even at 30% strain, reducing hysteresis loss close to zero. Use of EtOH as a solvent for AM monomer caused negative effects to mechanical and optical properties. Peel adhesion and repetitive cycle test results suggest that the relationship between peel adhesion and strain reversibility is inversely proportional. Optical feasibility was demonstrated through transmittance results. Moreover, the results of this study can propose a choice of acrylic monomers regarding a targeted purpose.

Chapter 3. Contact-induced molecular rearrangement

3.1 Experimental method and materials

Synthesis, peel adhesion test and rheological properties were conducted in accordance with 2.1 Experimental method and materials.

3.1.1 Characterization of surface properties

The adhesives were attached to the SUS substrate for a desired contact time prior to the contact angle measurement. Thereafter, the surface energy of the adhesives was calculated in accordance with the Fowkes theory using the contact angles of DI water and diiodomethane[29]. The contact angles of the droplets on the detached adhesives were measured using a drop shape analyzer (DSA100S, Kruss Gmbh, Germany). The calculated surface energy of the adherend was ~42.9 mJ m^{-2}. The measurement was performed at room temperature.

The surface functional groups of the synthesized PSAs (3MA and 3AA) were investigated by the Fourier-transform infrared (FTIR) technique (Varian 670-IR, Varian, the USA) using single-bounce attenuated total reflection (ATR) mode with N_2 gas purging. A germanium crystal was used as it has the lowest depth of penetration of 0.66 μm compared to that of the other materials. The FTIR spectra were recorded in absorption mode over the wavenumber range of 4000−650 cm^{-1}.

Time of flight secondary ion mass spectrometry (TOF-SIMS 5, IONTOF GmbH, Germany) was used to provide detailed molecular information about the surface of the synthesized PSAs. Each specimen was prepared with dimensions of 12 × 12 × 0.1 mm^3 and kept under an ultra-high vacuum of 10^{-9} mbar overnight before analysis. A 25 keV Bi^+ primary beam with 1 pA current was used to irradiate the sample for 300 sec over an area of 500 × 500 μm^2 for the surface analysis. The area of the spectra was calculated using Surfacelab 6 software.

3.2 Results and discussion

3.2.1 Peel adhesion test and contact angle measurement

Figure 3.1 shows the peel adhesion of 3MA and 3AA with respect to the contact time on the SUS substrate. The peel adhesion of 3MA remained practically constant with increasing contact time on SUS, whereas that of 3AA increased substantially (up to 300%). The former indicates that the peel adhesion of the methyl acrylate-incorporated PSAs is not contact time-dependent. The latter represents that the peel adhesion of the acrylic acid-containing PSAs is enhanced by the contact time. Since the rheological properties of the bulk are constant over time without external stimuli such as heat and UV light, the change in the surface properties must be a decisive factor contributing to the increased peel adhesion.

In order to understand the enhancement of the peel adhesion with variation of the contact time, the static water contact angles of the PSAs were measured. Figure 3.1(c) illustrates the difference in the contact angles of 3MA and 3AA with respect to the contact time on SUS. The contact angle of 3MA (~96.3±1°) was almost invariant, reflecting that its hydrophilicity was constant regardless of the contact time on SUS. In contrast, the contact angles of a DI water droplet on 3AA decreased with increasing contact time on SUS, suggesting that the surface of 3AA become more hydrophilic when subjected to

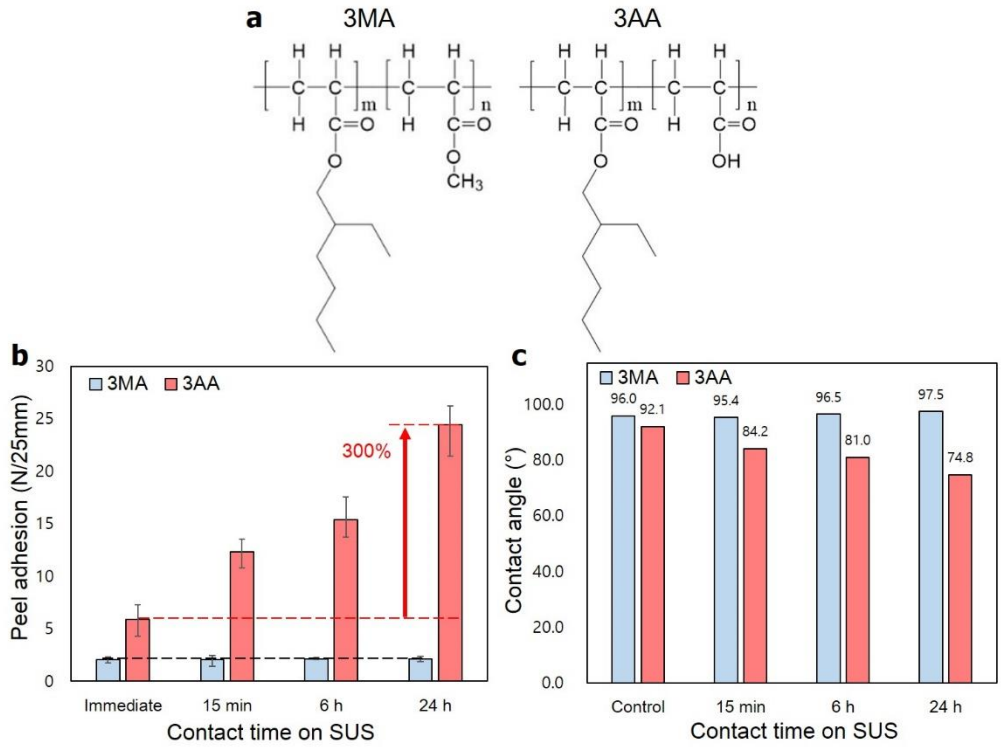

Figure 3.1 (a) Molecular structure of methyl acrylate- (3MA) and acrylic acid- (3AA) incorporated PSAs. (b) Peel adhesion of 3MA- and 3AA-incorporated PSAs. (c) Variation of contact angle of 3MA and 3AA with respect to contact time on SUS. The liquid used was DI water. 'Immediate' indicates around 10 sec of contact. The control represents the pristine PSAs before contact.

a longer contact time on the adherend. Since the peel adhesion of 3MA did not increase over time, with an indistinguishable contact angle change, the acrylate functionality is not a key factor despite its dipole moment. From the chemical point of view, the only difference between 3MA and 3AA is the existence of the acid functionality, which is expected to give rise to an enhancement of adhesion via hydrogen bonding. The surface energy of the PSAs was measured to prove enrichment of the hydrophilic groups in the vicinity of the surface. Figure 3.2 shows a visual representation of the change in the surface energy of each PSA with variation of the contact time on SUS, and the values are summarized in Table 1 and Table 2 for 3AA and 3MA, respectively. Figure 3.2 (a) shows an increase in the dispersive component within the first 15 min of contact, caused by an increase in the real contact area derived from wetting, followed by stabilization of the surface energy after 15 min of contact time. This increase does not effectively affect the peel adhesion (Figure 3.1 b). The observation suggests that the surface properties of the methyl acrylate-incorporated PSAs were practically unchanged with contact time. On the other hand, the total surface energy of 3AA increased continuously (even after the contact time of 15 min) when the adhesive was in prolonged contact with the SUS substrate (up to 24 h), attributed to increased exposure of polar components to the adherend (Figure 3.2 b), while the dispersive component remained almost constant. The previous reports suggest that the increase in peel adhesion, scaled as $\sim t^{1/2}$, can be diffusion-controlled process[30, 31]. Figure 3.2 (c) suggests that the enhancement of peel adhesion of 3AA can be divided into two regimes; regime I: the increase of real contact area, and regime II: a polymer chain rearrangement. Viscoelastic materials (PSAs) can flow once they come into adhesive contact so that the real contact area at the interface will increase with time[32], reflecting the slight increase of dispersive component of 3AA from the 'control' to '15 min' (Figure 3.2 b). This increase of the dispersive component can indicate more number of adhesive bonds, resulting in an increase of adhesion. And it can be dominant over the polymer chain rearrangement within 15 min contact time. The continuous increase of the polar component of 3AA (Figure 3.2 b) can be achieved via the polymer chain rearrangement at the interface, promoting the polar group exposure to the surface, thereby

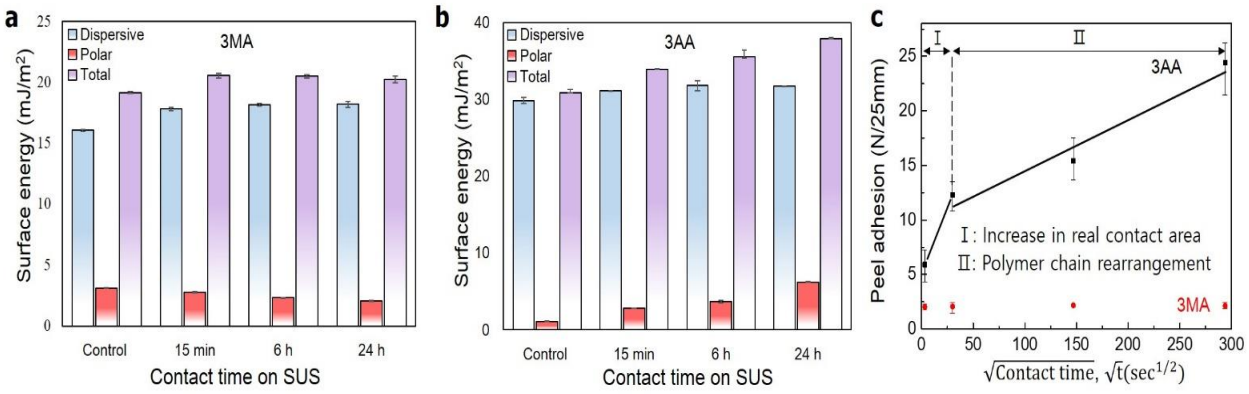

Figure 3.2 Surface energy of acrylic-monomer-based PSAs with respect to contact time on SUS: (a) 3MA and (b) 3AA. (c) Peel adhesion of 3AA and 3MA versus square root contact time.

increasing adhesion[33]. The most plausible polar group contributing to the increase in the polar component of 3AA is the acid group, meaning that this group is more prevalent at the interface of the adhesive subjected to a longer contact time on SUS. This result corresponds to the enhanced peel adhesion of 3AA with respect to the contact time on SUS. Thus, the presence of the polar group at the interface is the significant factor enhancing the peel adhesion.

Table 3.1 Surface energy and peel adhesion of acrylic-acid-incorporated PSAs (3AA) with respect to contact time on SUS.

Dwell time on SUS	3AA				
	Contact angle (°)		γ (mJ/m^2)		Peel adhesion (N/25mm)
	Water	Diiodomethane	γ^p	γ^d	
Control	92.1	57.8 ± 0.8	1.11±0.1	29.9±0.4	5.9±1.6
15 min	84.2	55.6 ± 0.1	2.81±0.1	31.1±0.1	12.3±1.5
6 h	81.0	54.3 ± 1.1	3.70±0.2	31.8±0.6	15.4±1.7
24 h	74.8	54.5 ± 0.2	6.23±0.1	31.7±0.1	24.4±2.3

Table 3.2 Surface energy and peel adhesion of methyl-acrylate-incorporated PSAs (3MA) with respect to contact time on SUS.

Dwell time on SUS	3MA				
	Contact angle (°)		γ (mJ/m^2)		Peel adhesion (N/25mm)
	Water	Diiodomethane	γ^p	γ^d	
Control	96.0	82.8±0.2	3.1±0.02	16.1±0.1	2.03±0.2
15 min	95.4	79.4±0.3	2.75±0.02	17.8±0.2	2.07±0.4
6 h	96.5	78.7±0.2	2.4±0.1	18.2±0.1	2.17±0.2
24 h	97.5	78.6±0.4	2.1±0.1	18.2±0.2	2.13±0.3

3.2.2 Surface analysis of the synthesized PSAs

In order to verify the enrichment of the acid groups on the surface via the molecular chain rearrangement of the polymer, surface analysis using FTIR and TOF-SIMS techniques was conducted. Unfortunately, the resolution of FTIR was not sufficient, and detailed surface investigation was unsuccessful, showing exactly the same spectra regardless of the contact time (Figure 3.3). The identical IR absorbance peaks of the individuals of organic functional groups can be attributed to the deep penetration depth of IR up to 0.66 μm, dominated by the bulk functionalities rather than the surface. Nevertheless, the TOF-SIMS data presented discriminative features depending on the contact time of 3AA on SUS, which is an antithetical result; no distinguishable changes observed on the acrylic acid-incorporated PSA's surface by XPS and SIMS subsequent to peeling out of the coatings containing urethane and acetate groups, as reported previously[34]. Figure 3.4 shows the spectra of the secondary negative ions produced by collision with the high-energy ion beam. Among these ions, the CHO_2^- ion (45 amu) is of interest, which is a fragment of the carboxylic acid functional groups contributing to the adhesion improvement. Thus, the signal at 45 amu was subjected to peak analysis for quantitative evaluation of the presence of the acid

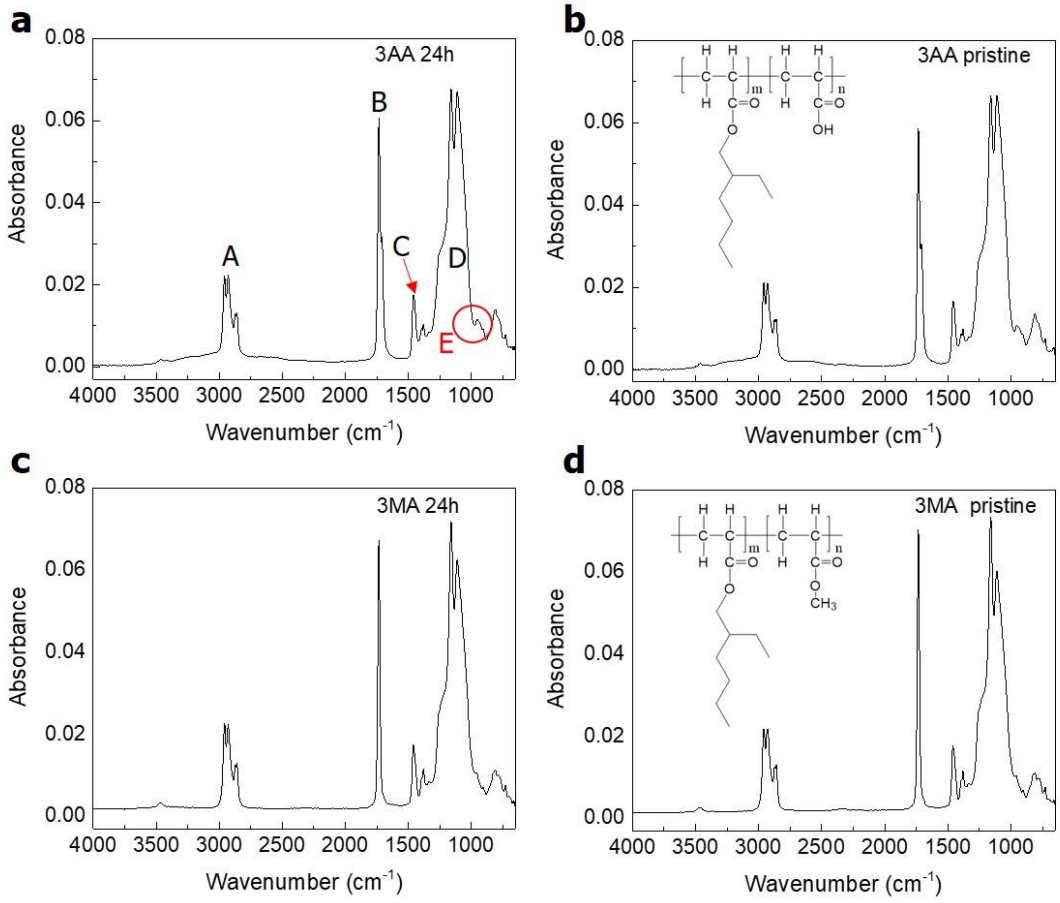

Figure 3.3 FTIR spectra of the synthesized acrylate-based PSAs with respect to contact time (a) 3AA 24 h, (b) 3AA control, (c) 3MA 24 h, and (d) 3MA control. The characteristic functional groups of the PSAs were detected at 3000−2900 cm^{-1}, 1733 cm^{-1}, 1458 cm^{-1}, and 1100 cm^{-1}, corresponding to C-H stretching, C=O stretching, CH_2 bending, and C-O-C stretching, respectively (labeled A, B, C and D, respectively).

group on the surface. The calculated area of the assigned peak of each specimen is noted in Figure 3.4 (c) and (i) for 3AA and 3MA, respectively. As expected, the area of the assigned peak for 3AA subjected to 24 h contact on SUS was 47% higher than that of the pristine sample. On the other hand, 3MA showed inconsequential difference between the signals of the 24 h contact time and pristine samples.

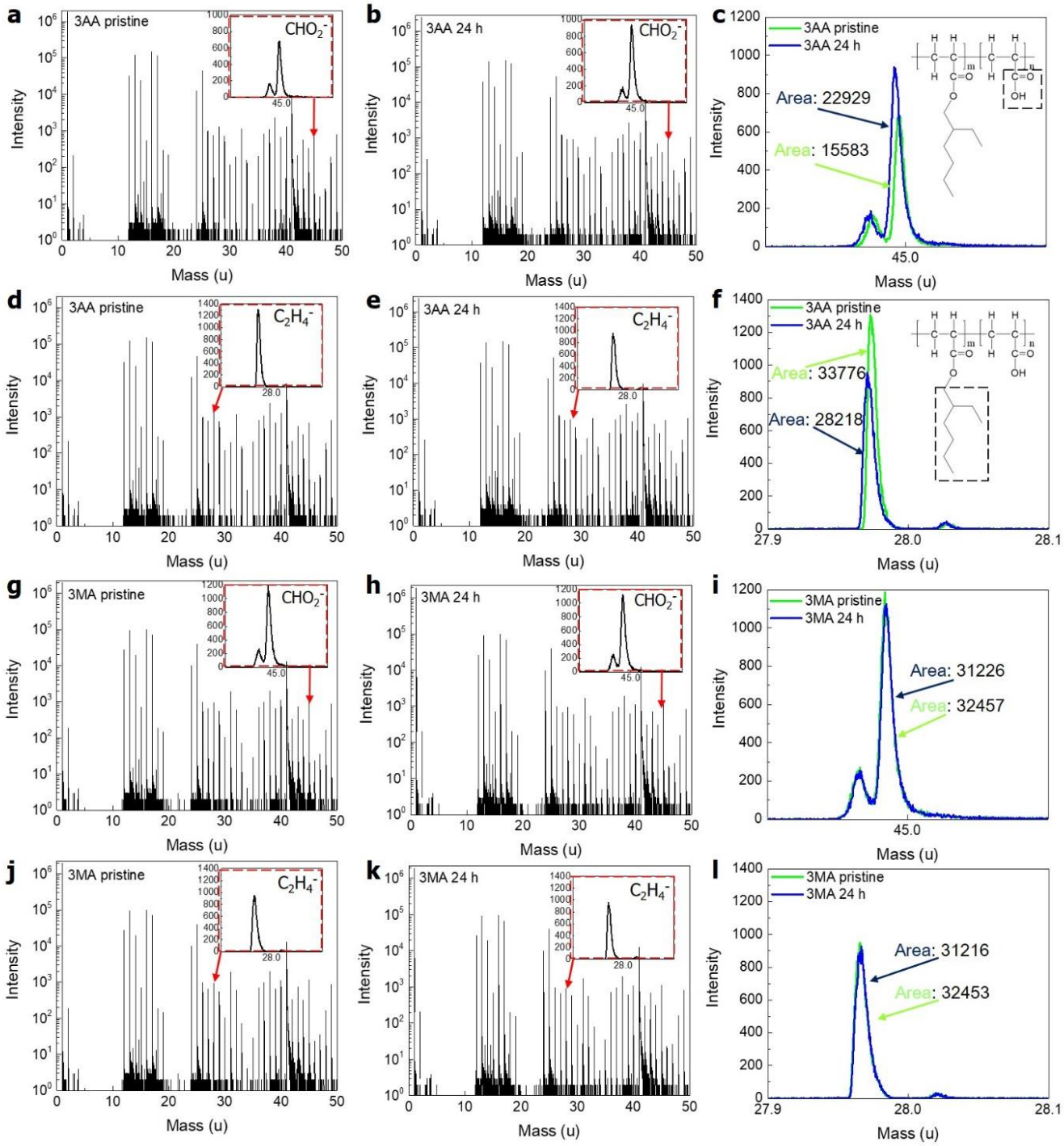

Figure 3.4 TOF-SIMS normal spectra of the synthesized PSAs with different metal contact times: (a) and (d) 3AA without contact, (b) and (e) 3AA with 24 h contact time, (c) comparison of the assigned peak, 45 mass, for a and b, (f) comparison of the assigned peak, 28 mass, for d and e, (g) and (j) 3MA without contact, (h) and (k) 3MA with 24 h contact time, (i) comparison of the assigned peak, 45 mass, for g and h and (l) comparison of the assigned peak, 28 mass, for j and k.

Notably, regardless of the contact time, the area of the assigned peak for 3MA was larger than that of 3AA. In addition, a peak at 45 amu was observed in the spectrum of 3MA, which is unexpected as this adhesive does not possess the carboxylic acid functionality. There are approximately 34 ion fragments with an atomic mass unit of 45, including SiO^-, $C_3H_9^-$, $C_2H_5O^-$, and $SiCH_5^-$. According to the principle of TOF-SIMS, the time taken for the accelerated ions to approach a detector is measured at a known distance, and the ions are resolved based on mass depending on this time. This means TOF-SIMS cannot distinguish chemically different substances with the same atomic mass. Thus, data acquisition at the assigned peak position may not only include CHO_2^- ions, but also the aforementioned ions with identical mass.

To elucidate the large difference of the peak intensity (Figure 3.4 c and i), storage moduli of 3AA and 3MA were measured (Figure 3.5). Hydrogen bonding formed between the acid moieties on the polymer chains of 3AA can provide stronger cohesion to its bulk, thereby increasing its modulus than that of 3MA which cannot have hydrogen bonding along the polymer chains. Consequently, at the constant analysis condition, 3AA can have fewer ion fragments than 3MA at the assigned peak 45. The comparable peak intensity of 3AA and 3MA at 28 amu (Figure 3.4 f and l) can be ascribed to the plenty of ethylhexyl-side-chains of the base monomer, 2-ethylhexyl acrylate (70 mol %) exposed to the surface. The highlight is that the area of the assigned peak was larger for 3AA subjected to 24 h contact with SUS than that of the pristine sample, and 3MA showed no significant changes under the same analysis conditions. This difference in the behavior of 3AA demonstrates the presence of more acid moieties on the surface, which is proof of molecular reorientation toward the metallic substrates.

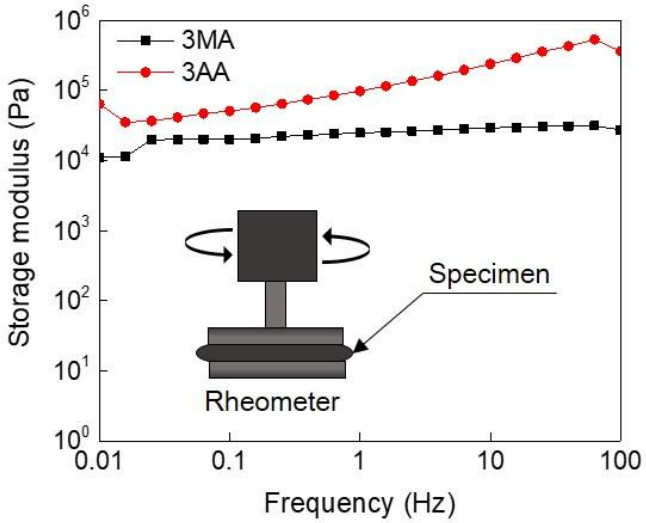

Figure 3.5 Storage modulus of the synthesized PSAs

Long ethylhexyl-groups, side chains of 2-EHA, are fragmented as subjected to the Bi^+ primary ion beam. A plausible fragment, $C_2H_4^-$ with 28 atomic mass unit, is assigned to evaluate the polymer chain rearrangement. A decrease of the peak intensity of 3AA (Figure 3.4 f) after 24 h of contact time suggests that the number of ethylhexyl-side-chains, primarily governing the vicinity of the surface, is reduced on the surface. By reflecting the almost constant dispersive component of 3AA with respect to the contact time, binding sites between the adherend and the adhesive are conserved. Thus, this intensity reduction indicates the replacement of the side chains with the acid groups via the polymer chain rearrangement. In contrast, the identical TOF-SIMS spectra of 3MA (Figure 3.4 l) represent its non-changeable surface properties over contact time.

3.2.3 Mechanism proposition

It is well known that the surface of SUS is covered with a chromium oxide layer that plays a major role in rust resistance. The carboxylic acid functional groups become thermodynamically more stable when these groups form hydrogen bonds with the metal oxide layer at the interface, as compared to their unassociated state. This thermodynamic driving force replaces the ethylhexyl-side-chains settled in previously with the acid groups via the molecular rearrangement and the reorientation of the acid groups on the polymer chains toward the interface (Figure 3.6). Subsequently, this oxide layer is able to spontaneously form hydrogen bonds with the carboxylic acid groups[35], substantially improving the adhesion of 3AA. Moreover, the long time-scale of the increase in the adhesion force (up to 24 h) indicates that the rearrangement process is mostly determined by rearrangement of the interfacial polymer chains, rather than single-bond rotation. Although Solid NMR is a powerful technique to directly prove hydrogen bonding[36], Solid NMR measurement was not feasible to confirm hydrogen bonding between carboxylic acid groups and the oxide layer of SUS because SUS powder exploited for the sampling purpose is magnetic-responsive due to ferrite derived from the processing, leading to the failure of Magic Angle Spinning.

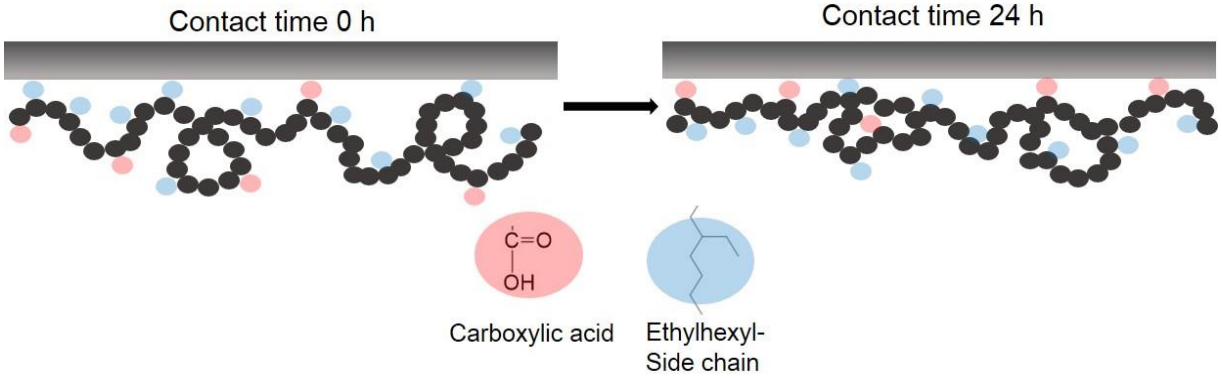

Figure 3.6 Schematic diagrams showing rearrangement of the polymer chains and reorientation of the acid moieties of 3AA toward the interface when the adhesive and the adherend are in contact.

In order to evaluate whether immersion of the PSAs in water can also induce an increase in the hydrophilicity, 3AA was dipped in DI water for 24 h instead of being subjected to contact with SUS. Figure 3.7 shows that the contact angle actually increased rather than decreased upon dipping (24 h). I suspect that dipping 3AA in DI water may wash away the residual acrylic acid monomers, leading to an increase in the hydrophobicity. This result manifests that DI water, despite its ability to form hydrogen bonds, is not suitable for inducing orientation of the polar groups (acid moieties) toward the surface. This may be caused by the failure of intimate contact between the water molecules and the adhesive at the interface due to the dominant hydrophobic alkyl chains on the surface of the adhesive.

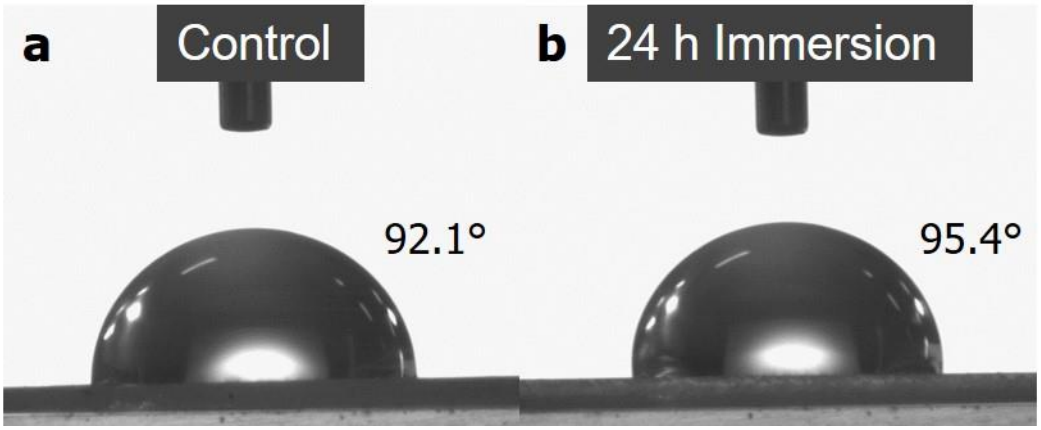

Figure 3.7 Contact angles of 3AA control (a) and after 24 h immersion in DI water (b). The control represents pristine PSA before contact.

3.3 Conclusions

The adhesion mechanism of lightly-crosslinked PSAs with acrylic acid (AA) and methyl acrylate was investigated with focus on the contact time-dependence of the polar functionality, which significantly improves the adhesion performance. The PSAs containing methyl groups presented constant peel adhesion regardless of the contact time, whereas the PSAs with the acrylic acid group displayed enhanced adhesion performance with increasing contact time. The measured contact angles and calculated surface energy suggest that an acrylic acid-rich surface can be achieved through contact with a metallic adherend over time. Sensitive surface analysis using TOF-SIMS verifies difference in the acid moieties on the surface of 3AA with respect to the contact time on SUS, clarifying the polymer chain rearrangement and molecular reorientation mechanism induced by the contact with the metallic adherend. These time-dependent changes led to further formation of strong interfacial hydrogen bonds, in addition to van der Waals interaction, between the adhesive and the metallic adherend. I demonstrate that the interfacial bonding triggered by the polymer chain rearrangement and molecular reorientation is the time-dependent mechanism by which peel adhesion of the adhesives is enhanced, and should be considered as an important factor for designing new types of PSAs.

Chapter 4. Compositional effect of acrylic acid

4.1 Experimental method and materials

Synthesis, peel adhesion test, rheological properties and transmittance measurement were conducted in accordance with 2.1 Experimental method and materials. The chemical compositions using acrylic acid (AA) and 2-ethylhexyl acrylate (EHA) are summarized in Table 4.1. All compositions have 15 wt. % of the fumed silica for viscosity control purpose.

Table 4.1 Molar percentage of comonomers used in the synthesis of acrylate-based PSAs

Compositions	EHA (mol %)	AA (mol %)
1AA	90	10
3AA	70	30
5AA	50	50
7AA	30	70

4.1.1 Stress relaxation and repetitive cycle tests

The stress relaxation and repetitive cycle tests were conducted using the universal testing machine (DAO-u1, DAO Technology, Republic of Korea) with dimensions of 13 × 38 mm^2 (W × L) at room temperature. For stress relaxation, specimens were subjected to variant strains from 1% to 300% and relaxed for 1 h. Plastic deformation was calculated, based on how long the specimens had to be elongated to obtain the same force as the initial after 60 min of the end of the test. For repetitive cycle test, the specimens were subjected to 25% strain with the crosshead speed of 500 mm/min. Hysteresis loss was calculated using numerical integration of the area between elongation and contraction curves.

4.1.2 Metal corrosiveness test

The synthesized PSAs were applied on ITO-coated glass substrates (AMGtech, Republic of Korea). The specimens were under hygrothermal condition at 50℃ and 90% relative humidity for 4 weeks. Surface resistance was measured using 4-point probe (CMT2000N, AIT, Republic of Korea). The average of surface resistance from five-different points of one specimen was reported.

4.1.3 Gel fraction measurement

The synthesized PSAs with dimensions of 13 × 25 mm^2 (W × L) were weighed (W_i) prior to immersion in tetrahydrofuran (THF) for 24 h at room temperature. The swollen PSAs were thoroughly dried for

24 h at room temperature, turning back to their original conformation. After drying, the PSAs were weighed (W_f), followed by determination of the gel fraction. The gel fraction of the synthesized PSAs was calculated in accordance with the following equation.

$$\text{Gel fraction } (\%) = (W_f / W_i) \times 100$$

where W_i and W_f are the initial weight and the weight after solvent immersion, respectively.

4.2 Results and discussion

4.2.1 Characterization of PSAs

First, I characterized thermal and mechanical properties of the prepared PSAs with respect to the various acrylic acid contents. As the molar ratio of acrylic acid increases from 10% to 70%, which represents 1AA, 3AA, 5AA and 7AA respectively, the PSAs exhibit higher rigidity. For example, the glass transition temperature of the PSAs increases with an increase of acrylic acid content (Figure 4.1 a), reflecting less molecular mobility such as bond rotation at room temperature in accordance with Free volume theory. An increase of acrylic acid content indicates the increment of intermolecular forces between polymer chains, which is derived from an increase of hydrogen bonding sites. This restriction hinders molecular motions, resulting in high T_g. This hindrance of the molecular movement resulting in rigidity is congruous with the mechanical behavior of the specimens, becoming stiffer as more acrylic acid is incorporated (Figure 4.1 b).

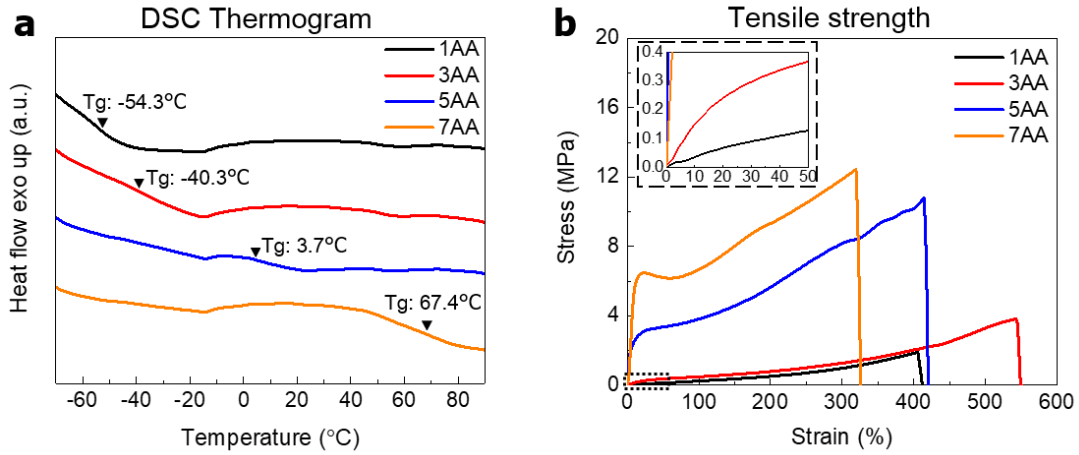

Figure 4.1 (a) DSC thermogram and (b) typical stress-strain curve of the acrylic acid-incorporated PSAs with respect to different chemical compositions.

Figure 4.2 shows peel adhesion of the PSAs with different chemical compositions. While 5AA and 7AA displayed almost 'zero' peel adhesion, 1AA and 3AA exhibited the high peel adhesion as ~ 13.7 N/25mm, which is approximately 65% higher than the peel adhesion (8.34 N/25mm) of widely used 'Scotch tape' (PK65 48×40 Transparent, 3M, USA)[7]. The wetting images and rheological properties of

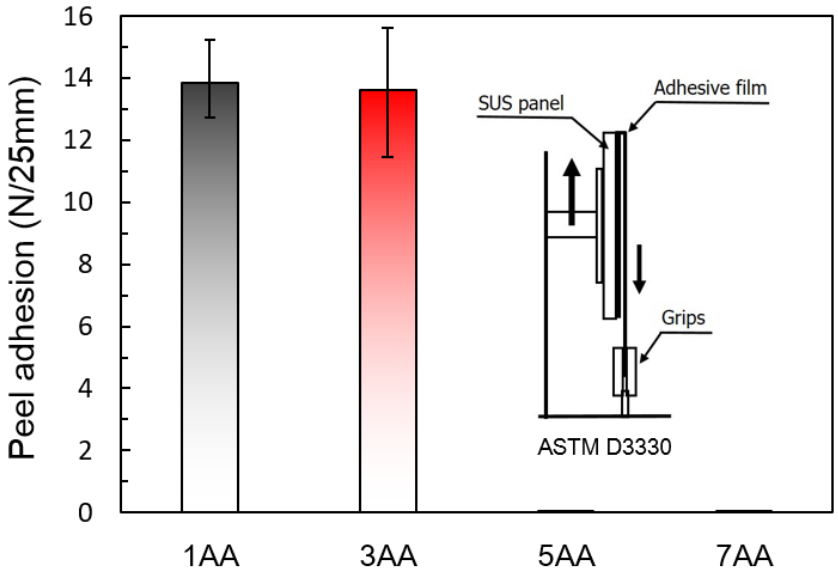

Figure 4.2 Peel adhesion of the acrylic acid-incorporated PSAs with respect to different chemical compositions.

the acrylic acid-incorporated PSAs were implemented to explicate the relation between acrylic acid contents and peel adhesion. All adhesives must achieve intimate wetting with substrates to maximize their adhesion performance. Since PSAs behave more like soft solids than like liquids during the wetting process, their wettability is governed by the modulus, i. e. lower modulus promotes wetting[23]. Even though the adhesive wets and forms interfacial bonds with the substrate, the adhesive would not perform its function if it could not resist fracture and debonding. Consequently, fracture toughness of adhesives

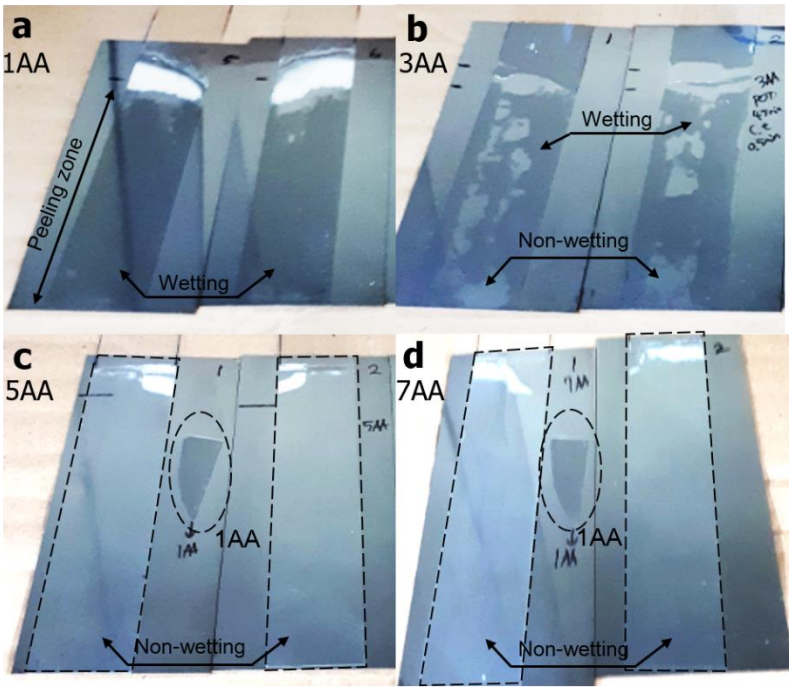

Figure 4.3 Wetting images of the acrylic acid-incorporated PSAs with respect to different chemical compositions: (a) 1AA, (b) 3AA, (c) 5AA and (d) 7AA. 1AA in (c) and (d) was attached for wetting comparison purpose.

is an important property and it depends on the ability of the adhesive to dissipate energy by a yielding deformation near the crack tip[23]. Generally, loss modulus (G") measurement is employed to indicate how much energy is absorbed through deformation during peeling[22]. Figure 4.3 suggests that addition of more acrylic acid is detrimental to wettability of the adhesives as subjected to contact with SUS. Storage moduli (Figure 4.4) of the prepared PSAs support a propensity of the wettability based on the aforementioned explanation. It shed light on a criterion for intimate wetting of the PSA in this system, which a PSA should have storage modulus less than 55 kPa at 1 Hz. Regarding the loss moduli (Figure 4.4) of the PSAs, 3AA should have shown the higher peel adhesion than 1AA. The recent study demonstrated that acrylic acid-incorporated PSAs enable strong interfacial bond formation induced by the contact with the metallic adherend through molecular reorientation and polymer chain rearrangement [37]. It suggests that the reason why 3AA has the comparable peel adhesion with 1AA is due to 'non-wetting' spots of 3AA, reducing total contact area despite its more acid moieties (30 mol%) which offer more chances to form strong interfacial bonds with SUS. It leads to the primary conclusion that an intimate wetting or contact between an adhesive and an adherend is a prerequisite for high adhesion performance unless the adhesive behaves like liquids, which can be modulated through acrylic acid content. 1AA was adopted to investigate its viscoelastic properties as well as to evaluate its eligibility for wide range of electronic applications since it exhibited the best adhesion performance among the compositions in terms of wetting and peel adhesion.

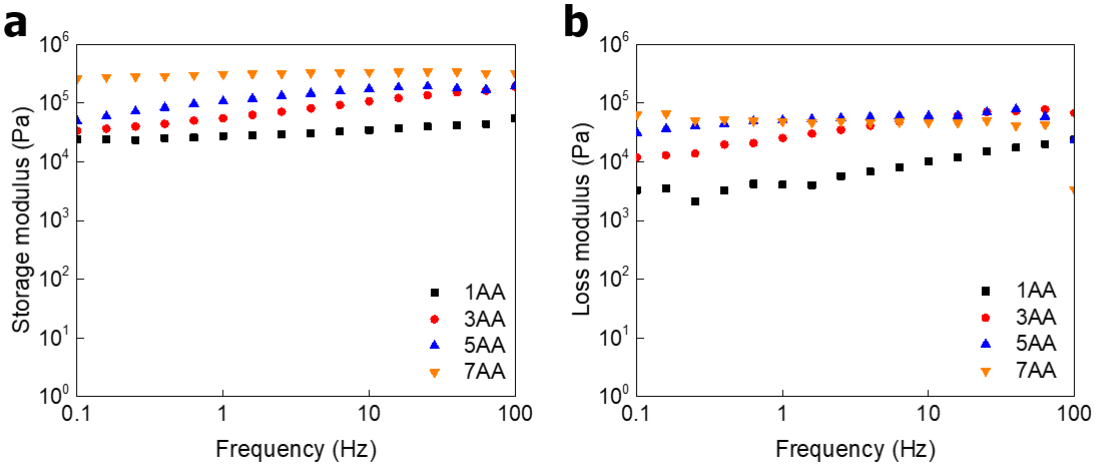

Figure 4.4 Rheological properties of the acrylic acid-incorporated PSAs with respect to different chemical compositions; (a) storage modulus and (b) loss modulus. Storage modulus order of PSAs at 1Hz: 7AA (308 kPa) > 5AA (107 kPa) > 3AA (55 kPa) > 1AA (27 kPa).

4.2.2 Stress relaxation and repetitive cycle test

Figure 4.5 shows the results of stress relaxation of 1AA with respect to various strains. In the stress relaxation test, the stress was measured at given strains and at the constant temperature as a function of time. Notably, no macroscopic movement of the specimen can occur because the strain after stretching is unchangeable. Consequently, stress relaxation can take place on molecular level. There are several

mechanisms explaining relaxation processes such as viscous flow, molecular relaxation and disentanglement or bond-interchange (e.g., vitrimer) of physical crosslinks[38]. These processes are in such a way as to reach an equilibrium under the stress[39]. Since percolation network is established in 1AA using HDDA, viscous flow caused by linear polymer chains slips is not favorable. Hence, the plausible relaxation process can be designated to molecular relaxation motions.

Figure 4.5 (a) shows the results of stress relaxation of 1AA with respect to various strains as a function of time. A measure of stress fraction was achieved by dividing the stress at time t (σ_t) by the maximum stress (σ_i), the reference stress. The time zero (0 sec) was set as the time at which the maximum stress

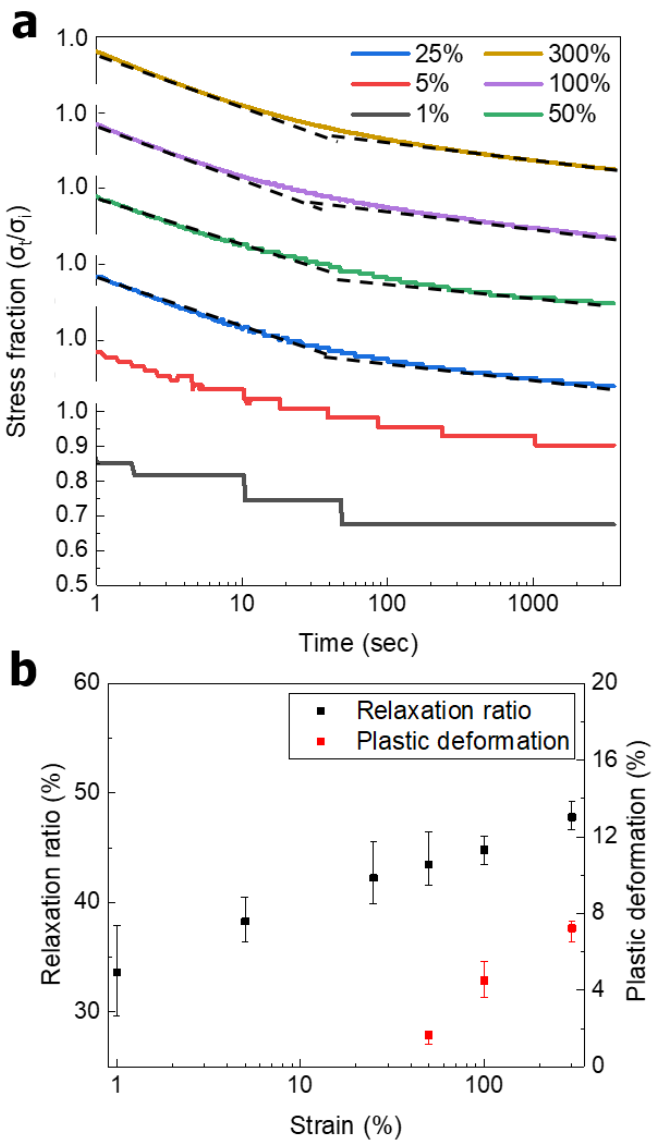

Figure 4.5 Stress relaxation of 1AA at various strains: (a) semilogarithmic plot of 1AA at different strains. σ_i represents the maximum stress and σ_t indicates the stress at time t, and (b) calculated relaxation ratio and plastic deformation of 1AA with respect to strains. The given values are the average of at least three repetitions. The stair-like stress-time curves of 1AA at 1% and 5% is attributed to the resolution issue of the 10kgf loadcell in addition to the low stiffness of 1AA, limiting the linear fitting.

of the specimens was obtained. The experimental results appear to consist of two straight lines; the greater slope of the early line is laid for times less than about 1 min and the smaller for greater times, which is corresponding to the stress against logarithmic time scale of the carbon black-reinforced natural rubber composites[40]. The regimes distinguished by two linear sections imply two distinct relaxation mechanisms of the fumed silica-reinforced adhesives. Stress relaxation of a crosslinked polymer network was proposed to occur via a retracting mechanism (a concept of reptation) in which the unassociated chain ends (or dangling chain) diffuses toward the chain ends which are attached to the network[41, 42]. The breakdown of the filler structure was suggested to describe the first relaxation process of the filler-reinforced rubber vulcanizates[40]. From these proposed relaxation mechanisms, I postulate that viscoelastic relaxation of 1AA can be attributed to the breakdown of the structure built from the fumed silica particles which is dominant within first 1 min of relaxation, followed by retracting free chain ends toward the chain ends which are associated with the network.

Stress relaxation ratio and plastic deformation of 1AA with respect to various strains is shown in Figure 4.5 (b), and its pictures after the test are shown in Figure 4.6. The results indicate that relaxation ratio and plastic deformation are proportional to strains. It is generally known that the elasticity of

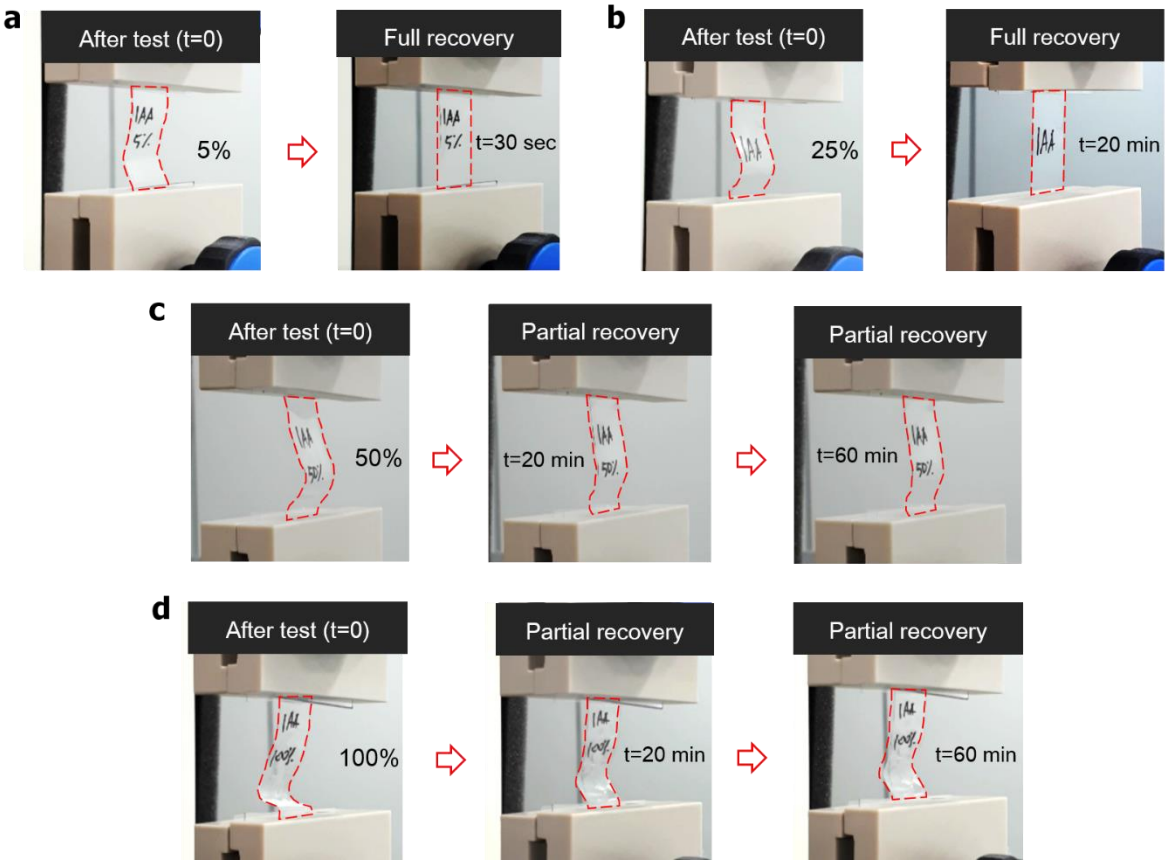

Figure 4.6 Specimens straightly after stress relaxation test (t=0) at (a) 5% strain, (b) at 25% strain, (c) at 50% strain, (d) at 100% strain. 300% strained specimens showed worse recovery than that of 100% strain.

rubber is driven by entropy change. It is worth noting that elastic behavior is immediate and reversible, which is thermodynamic, however recoverable deformation is time dependent, which is kinetics[24]. To elucidate the results of relaxation ratio and plastic deformation at given strains, relaxation process is speculated based on thermodynamics, statistical theory of rubber elasticity and a concept of reptation in a polymer chain point of view. The filler-structure breakdown mechanism is excluded in the following explanation because this relaxation process is believed to be governing at an initial stage.

As strained, the conformation of the polymer network changes from random coil to the linear state, providing tensile stress. This mechanical stress can be sufficient to trigger vigorous motions of polymer chains, resulting in the break of intermolecular forces (e.g., van der Waals forces and hydrogen bonds). This movement can lead to segmental rearrangement, causing retraction of dangling chains because 1AA is in a rubbery state at room temperature, implying plenty of free volume as evidenced by its low T_g (Figure 4.1 a). This entire process results in stress relaxation (Figure 4.7). The retracted chains will give rise to an increase of entropy of the polymer network at the fixed strain due to their non-linear conformation, followed by an equilibrium shift as returning to the origin, i. e., a thermodynamically stable state can be achieved at a higher strain rather than zero strain, resulting in the partial recovery and plastic deformation. Or it can be obtained through balancing between the entropic restoring force and the restraining force formed by reversible hydrogen bond. An increase of relaxation ratio with increasing strains manifests more active segmental rearrangement of polymer chains at higher stress.

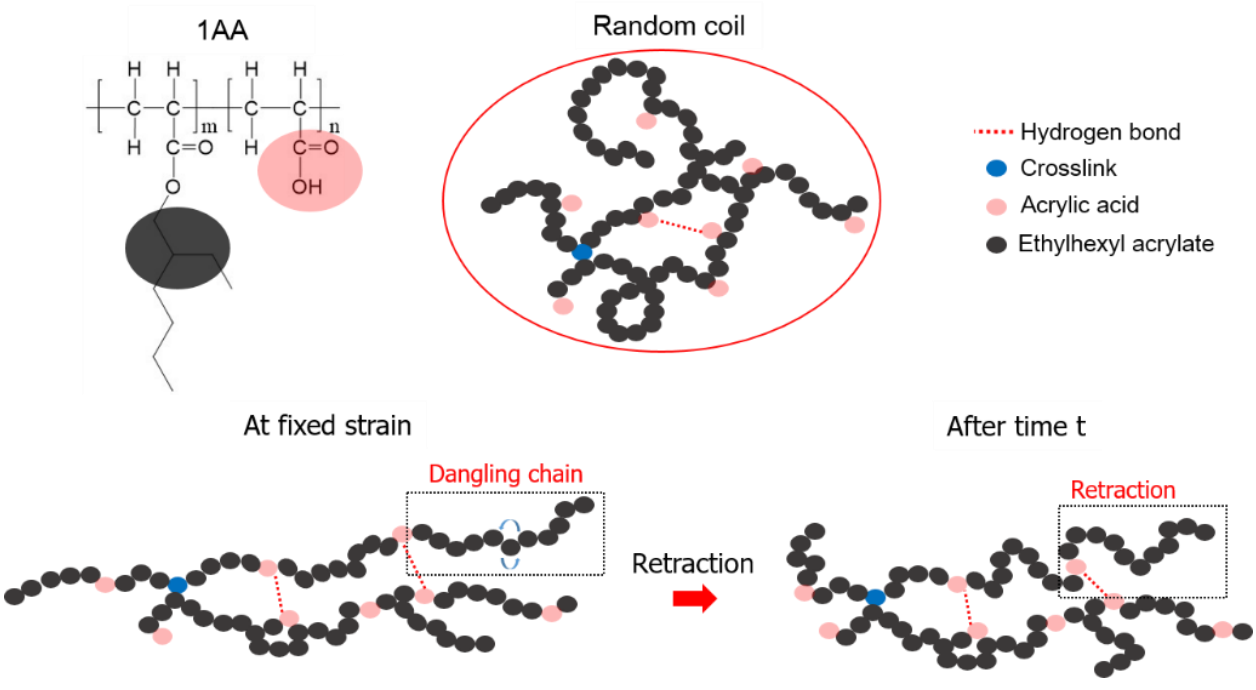

Figure 4.7 Schematic diagrams of 1AA during stress relaxation

All specimens equal or less than 25% strains exhibited the full recovery although the recovery time is dependent on the strain (Figure 4.6 a and b). On the other hand, partial recovery was obtained from the specimens with strains higher than 25%. No further recovery was observed after 20 min (t=20 min) of the stress relaxation test from these specimens (Figure 4.6 c and d). Figure 4.6 (a) and (b) signify the conserved degree of disorder to a certain extent despite elongation, which enables full recovery according to thermodynamics of rubber elasticity. The temporal difference of Figure 4.6 (a) and (b) suggests that acid moieties in 1AA can have more chances to build up the reversible hydrogen bond formation as strained more highly, resulting in the stronger hindrance against retraction. This speculation can be driven by shorter inter-chain distance based on the description of Poisson ratio of polymeric materials, representing the perpendicular contraction to the longitudinal elongation[43]. The plausible explanation for the way to relieve the stress at the short strains by conserving the chain disorder is relaxation through bond rotation of alkyl-side chains (or ethylhexyl side chains).

There are three conditions to achieve rapid strain reversibility[24]. First, the polymeric materials should be amorphous to make strain reversibility thermodynamically favored. Second, there should be minimum number of intermolecular forces hindering the polymer chain retraction. Lastly, crosslinking is requisite to provide percolation network, preventing relative translational motion. All of these criteria can lead to elastomer-like performance which minimizes energy loss as heat during elongation and contraction. Stress-strain response of 1AA against dynamic or repetitive mechanical stimulus is shown in Figure 4.8. Total strain of 25% was chosen based on the stress relaxation results, showing full recovery of the specimen. It was found that approximately two minutes were taken for full recovery (Figure 4.8 e) after a set of 100-cycle test, which is around 10 times shorter than that of the obtained from the stress relaxation test at the same strain. It can be ascribed to the shorter dwell time at the maximum strain, limiting the formation of new hydrogen bond among polymer chains. 10 sets of sequential repetitive 100-cycle test after 2 min of interval certify that 1AA is able to retain conformational recovery as well as constant mechanical properties (Figure 4.8 e). Nonetheless, the recovery time must be minimized for user convenient purpose. For instance, if contemporary devices such as flexible smart watches and foldable mobile phones (e.g., SAMSUNG Galaxy Fold and HUAWEI Mate X) were not able to achieve rapid strain reversibility, wrinkles and wavy surface would have been remained on display, leaving discomforts to users. Hence, I implemented ‘pre-strain’ strategy in order to accomplish instantaneous strain reversibility as subjected to 15% strain. Figure 4.8 (f) displays stress-strain curves of 1AA with 10% pre-strain for 100-cycle test. Practically identical hysteresis loss over the cycles reflects its elastomer-like behavior[7].

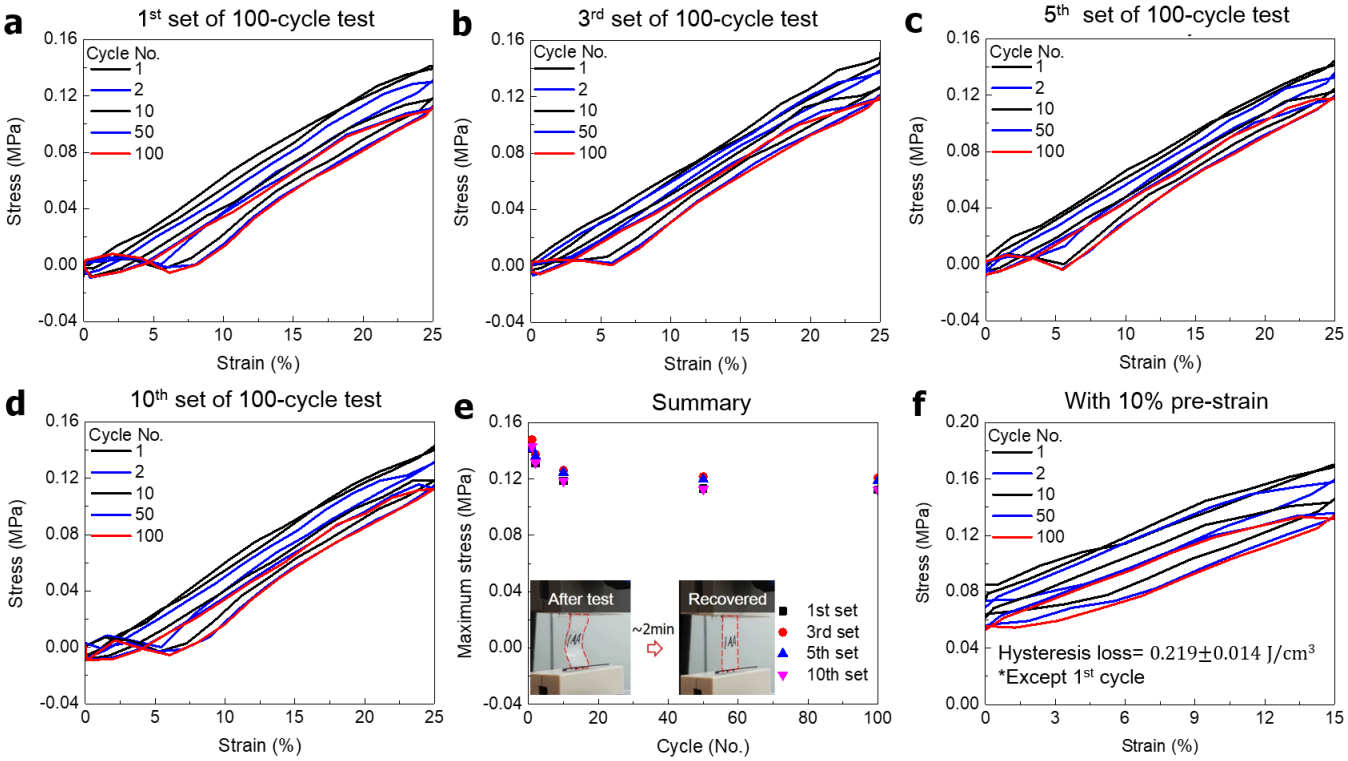

Figure 4.8 Repetitive cycle test of 1AA; (a) 1st set, (b) 3rd set, (c) 5th set, (d) 10th set, (e) summary of maximum stress at each cycle number and (f) stress-strain curves of 1AA with 10% pre-strain out of 25% total strain. Each set consists of 100-cycle. 2 min of interval for full recovery was given after each sequential test set.

4.2.3 Evaluation for device applications

Transmittance measurement (%T) of PSAs with respect to variant acrylic acid contents is available in Figure 4.9 (a). Light transmittance decreases with an increase of acrylic acid content. This is because the more acid moieties enable strong interaction through the formation of hydrogen bond among polymer chains, increasing crystallinity. It results in a decrease of light transmittance and this explanation is evidenced by the appearance of polyacrylic acid which is a white solid. Figure 4.9 (b) shows transmittance measurement of 1AA. It exhibits high transmittance (> 90 %T) over the visible light range as strained up to 30%, meaning that 1AA is highly transparent during repetitive-cyclic motion with rapid retraction given by 'pre-strain'. The reason why %T declines as strain increases can be attributed to the change of polymer structure (i.e., random coil to linear chain), possibly increasing crystallinity or the fluctuation of the filler network derived from filler reorientation or alignment.

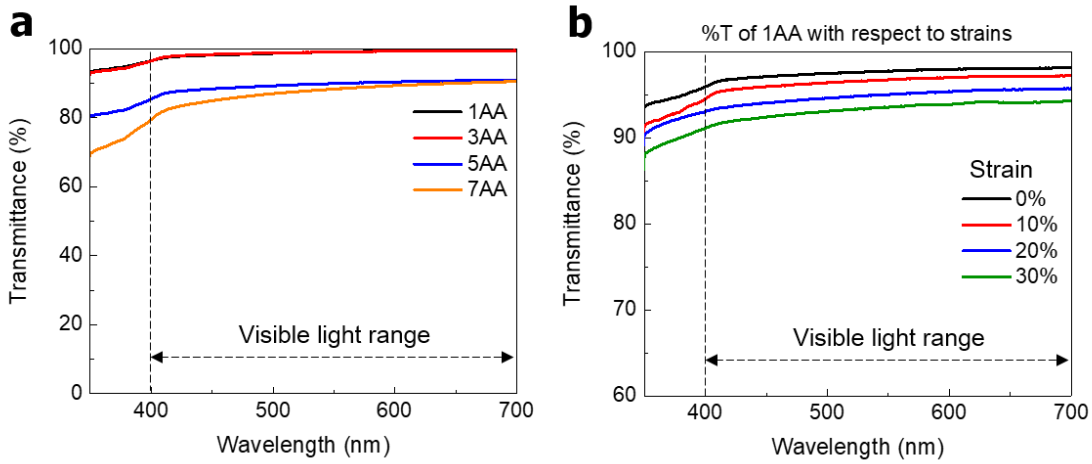

Figure 4.9 Transmittance measurement (%T) of acrylic acid-incorporated PSAs: (a) %T of the PSAs with respect to variant acrylic acid contents and (b) 1AA strained up to ~ 30%.

Although the acrylic acid containing PSAs are generally known for their excellent adhesion performance, some reports have described that carboxylic acid implemented soft adhesives can cause corrosion to metal substrates[9, 44]. To evaluate the compatibility of 1AA with the corrosion sensitive layer (ITO, indium tin oxide), 1AA and 1MA composed of 10 mol % of methyl acrylate were applied on ITO-coated glass substrates for 4 weeks under the hygrothermal condition. 1MA was employed for the acid effect comparison. Surface resistance of ITO substrates covered by PSAs is shown in Figure 4.10. It is obvious that the surface resistance is invariant as compared to 'As-received' regardless of functional groups (carboxylic acid or methyl group) as a function of exposing time when it is conditioned at 50℃ and 90% relative humidity, representing compatibility of 1AA with the corrosion sensitive layer. This result surpasses the outcome of the US patent in electrical resistance consistency of ITO after aging[45]. The underlying mechanism for ITO corrosion is from contamination due to impurities[46]. Metal corrosion robustness of 1AA can be related to its high gel fraction (99.2±0.5%), hardly leaving residual acrylic acid on ITO substrates. This evaluation demonstrates eligibility of 1AA for wide range of

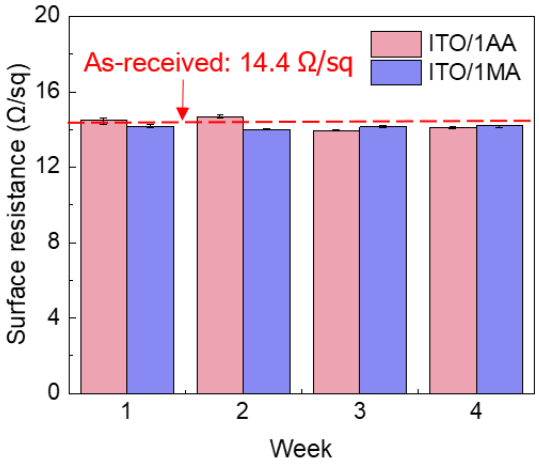

Figure 4.10 Surface resistance of ITO covered by 1AA and 1MA with respect to exposing time (weeks) when it is conditioned at 50℃ and 90% relative humidity.

electronic devices with advanced properties.

4.3 Conclusions

Physical properties of PSAs with variant acrylic acid contents were successfully characterized. The results represent that more acrylic acid compositions render PSAs stiffer and more translucent, leading to poor adhesion performance as well as unfavorable wetting on the substrate. Concerning adhesion performance, the PSA with 10 mol% acrylic acid incorporation was adopted for viscoelastic test and evaluation for electronic device application. Under the static stimulus, it was found that the trend of relaxation ratio is strain-dependent, suggesting vigorous polymer chain motions at high strains. In addition, its viscous component becomes dominant as subjected to higher strains, which is quantitatively estimated through plastic deformation calculation. Conformational and mechanical recoveries of the designated PSA emphasize its advantage for stretchable adhesive design. Plus, pre-strain strategy enables instantaneous strain reversibility. The evaluation substantiates high optical clarity as strained and excellent compatibility of the acrylic acid-containing PSA with the corrosion sensitive layer. Our results provide design guidelines to achieve both relaxation and recovery with high adhesion performance and metal corrosion robustness, which cause positive contribution to the development of advanced adhesives for contemporary device application.

Chapter 5. Summary

Acrylate-based PSAs were synthesized through UV curing, and their physical properties with respect to various acrylic monomers and compositions were successfully characterized. Concerning monomer functionality effect, AA incorporation showed the highest peel adhesion among others (-CH_3, -OH and -NH_2) and this result was explained through energy dissipation principles with an aid of loss modulus (G''). Instantaneous strain reversibility was achieved through the formulation using MA and HEA, indicating the relationship between adhesion and reversibility is inversely proportional. Use of EtOH as a solvent for AM monomer caused detrimental effects to mechanical and optical properties, probably because of its poor solubility in the monomer mixture after drying EtOH during processing. Compositional effect of acrylic acid monomer exhibited that the more acrylic acid implementation rendered the synthesized PSAs stiffer, resulting in poorer adhesion performance attributed to the failure of intimate wetting. Rheological data of all compositions suggest that there is an optimized storage modulus facilitating intimate wetting with the substrate. Stress relaxation of 1AA displayed its viscoelastic properties; strain-dependent relaxation ratio and viscous component were achieved, and these properties were interpreted on microscopic level based on conventionally proposed thermodynamics of rubber elasticity and the stress relaxation mechanism. Repetitive cycle test with pre-strain strategy and the evaluation for device applications (light transmittance and metal corrosion robustness) clearly demonstrated its eligibility as advanced adhesives employed for stretchable/flexible display assembly. Additionally, molecular rearrangement and reorientation which are triggered by the contact with a metallic adherend underlay the enhancement of peel adhesion of acrylic acid-incorporated PSAs.

References

1. Kim, D.-H.; Lu, N.; Ma, R.; Kim, Y.-S.; Kim, R.-H.; Wang, S.; Wu, J.; Won, S. M.; Tao, H.; Islam, A.; Yu, K. J.; Kim, T.-i.; Chowdhury, R.; Ying, M.; Xu, L.; Li, M.; Chung, H.-J.; Keum, H.; McCormick, M.; Liu, P.; Zhang, Y.-W.; Omenetto, F. G.; Huang, Y.; Coleman, T.; Rogers, J. A., Epidermal Electronics. *Science* **2011,** *333* (6044), 838.

2. Koo, J. H.; Kim, D. C.; Shim, H. J.; Kim, T.-H.; Kim, D.-H., Flexible and Stretchable Smart Display: Materials, Fabrication, Device Design, and System Integration. *Advanced Functional Materials* **2018,** *28* (35), 1801834.

3. Lim, S.; Son, D.; Kim, J.; Lee, Y. B.; Song, J.-K.; Choi, S.; Lee, D. J.; Kim, J. H.; Lee, M.; Hyeon, T.; Kim, D.-H., Transparent and Stretchable Interactive Human Machine Interface Based on Patterned Graphene Heterostructures. *Advanced Functional Materials* **2015,** *25* (3), 375-383.

4. Krishnan, S. R.; Su, C.-J.; Xie, Z.; Patel, M.; Madhvapathy, S. R.; Xu, Y.; Freudman, J.; Ng, B.; Heo, S. Y.; Wang, H.; Ray, T. R.; Leshock, J.; Stankiewicz, I.; Feng, X.; Huang, Y.; Gutruf, P.; Rogers, J. A., Wireless, Battery-Free Epidermal Electronics for Continuous, Quantitative, Multimodal Thermal Characterization of Skin. *Small* **2018,** *14* (47), 1803192.

5. Kirihara, O., Optically Clear Adhesives and Bonding Technology. S&T publishing, Tokyo: 2012.

6. Yi, D., Touch Panel Report-OCA/OCR for Touch Panel-2013, IHS. **2013**.

7. Lee, J. H.; Myung, M. H.; Baek, M. J.; Kim, H.-S.; Lee, D. W., Effects of monomer functionality on physical properties of 2-ethylhexyl acrylate based stretchable pressure sensitive adhesives. *Polymer Testing* **2019,** *76*, 305-311.

8. Lee, J.-G.; Shim, G.-S.; Park, J.-W.; Kim, H.-J.; Han, K.-Y., Kinetic and mechanical properties of dual curable adhesives for display bonding process. *International Journal of Adhesion and Adhesives* **2016,** *70*, 249-259.

9. Park, C.-H.; Lee, S.-J.; Lee, T.-H.; Kim, H.-J., Characterization of an acrylic polymer under hygrothermal aging as an optically clear adhesive for touch screen panels. *International Journal of Adhesion and Adhesives* **2015,** *63*, 137-144.

10. Creton, C., Pressure-sensitive adhesives: an introductory course. *Materials Research Society Bulletin* **2003,** *28* (6), 434-439.

11. Ishikawa, N.; Furutani, M.; Arimitsu, K., Pressure-sensitive adhesive utilizing molecular interactions between thymine and adenine. *Journal of Polymer Science Part A: Polymer Chemistry* **2016,** *54* (10), 1332-1338.

12. Czech, Z., Synthesis and cross-linking of acrylic PSA systems. *Journal of Adhesion Science and Technology* **2007,** *21* (7), 625-635.

13. Satas, D., *Handbook of pressure sensitive adhesive technology*. Van Nostrand Reinhold New York: 1989; Vol. 1.

14. Czech, Z.; Kowalczyk, A.; Kowalska, J., Photoreactive UV-Crosslinkable Pressure-Sensitive Adhesives Based on Butyl Acrylate and 4-Acryloyloxy Benzophenone Copolymers. *Journal of Research Updates in Polymer Science* **2013,** *1* (2), 96-100.

15. Kayaman-Apohan, N.; Demirci, R.; Cakir, M.; Gungor, A., UV-curable interpenetrating polymer networks based on acrylate/vinylether functionalized urethane oligomers. *Radiation Physics Chemistry* **2005,** *73* (5), 254-262.

16. Felekoğlu, B.; Tosun, K.; Baradan, B.; Altun, A.; Uyulgan, B. J. C.; research, c., The effect of fly ash and limestone fillers on the viscosity and compressive strength of self-compacting repair mortars. **2006,** *36* (9), 1719-1726.

17. Park, Y.-J.; Lim, D.-H.; Kim, H.-J.; Park, D.-S.; Sung, I.-K., UV-and thermal-curing behaviors of dual-curable adhesives based on epoxy acrylate oligomers. *International Journal of Adhesion and Adhesives* **2009,** *29* (7), 710-717.
18. Sun, S.; Li, M.; Liu, A., A review on mechanical properties of pressure sensitive adhesives. *International Journal of Adhesion Adhesives* **2013,** *41*, 98-106.
19. Creton, C.; Ciccotti, M., Fracture and adhesion of soft materials: a review. *Reports on Progress in Physics* **2016,** *79* (4), 046601.
20. Peykova, Y.; Lebedeva, O. V.; Diethert, A.; Müller-Buschbaum, P.; Willenbacher, N., Adhesive properties of acrylate copolymers: Effect of the nature of the substrate and copolymer functionality. *International Journal of Adhesion and Adhesives* **2012,** *34*, 107-116.
21. Luo, W.; Hu, X.; Wang, C.; Li, Q., Frequency-and strain-amplitude-dependent dynamical mechanical properties and hysteresis loss of CB-filled vulcanized natural rubber. *International Journal of Mechanical Sciences* **2010,** *52* (2), 168-174.
22. Mazzeo, F. A., Characterization of pressure sensitive adhesives by rheology. *TA Instruments report RH082* **2002**, 1-8.
23. Yarusso, D. J., *Adhesion Science and Engineering—The Mechanics of Adhesion*. Elsevier, Amsterdam: 2002; Vol. 1, p 499-533 Ch. 13.
24. Shanks, R. A.; Kong, I., General purpose elastomers: structure, chemistry, physics and performance. In *Advances in Elastomers I*, Springer: 2013; pp 11-45.
25. Bower, D. I., Mechanical properties I – time-independent elasticity. In *An Introduction to Polymer Physics*, Cambridge University Press: Cambridge, 2002; pp 162-186.
26. Falsafi, A.; Tirrell, M.; Pocius, A. V., Compositional effects on the adhesion of acrylic pressure sensitive adhesives. *Langmuir* **2000,** *16* (4), 1816-1824.
27. Yamaguchi, K.; Busfield, J. J. C.; Thomas, A. G., Electrical and mechanical behavior of filled elastomers. I. The effect of strain. *Journal of Polymer Science Part B: Polymer Physics* **2003,** *41* (17), 2079-2089.
28. Song, W. J.; Park, J.; Kim, D. H.; Bae, S.; Kwak, M. J.; Shin, M.; Kim, S.; Choi, S.; Jang, J. H.; Shin, T. J., Jabuticaba-Inspired Hybrid Carbon Filler/Polymer Electrode for Use in Highly Stretchable Aqueous Li-Ion Batteries. *Advanced Energy Materials* **2018,** *8* (10), 1702478.
29. Rulison, C., So you want to measure surface energy. *Kruss Technical Note #306, Kruss USA* **1999**, 1-16.
30. Lee, D. W.; Lim, C.; Israelachvili, J. N.; Hwang, D. S., Strong Adhesion and Cohesion of Chitosan in Aqueous Solutions. *Langmuir* **2013,** *29* (46), 14222-14229.
31. Banquy, X.; Kristiansen, K.; Lee, D. W.; Israelachvili, J. N., Adhesion and hemifusion of cytoplasmic myelin lipid membranes are highly dependent on the lipid composition. *Biochimica et Biophysica Acta (BBA) - Biomembranes* **2012,** *1818* (3), 402-410.
32. Israelachvili, J. N., 17 - Adhesion and Wetting Phenomena. In *Intermolecular and Surface Forces (Third Edition)*, Israelachvili, J. N., Ed. Academic Press: San Diego, 2011; pp 415-467.
33. Mortazavi, M.; Nosonovsky, M., A model for diffusion-driven hydrophobic recovery in plasma treated polymers. *Applied Surface Science* **2012,** *258* (18), 6876-6883.
34. Kinning, D. J., Surface and interfacial structure of release coatings for pressure sensitive adhesvies. *Proceedings of the Adhesion Society* **1995**, 288.
35. Chehimi, M. M.; Azioune, A.; Cabet-Deliry, E., Acid-base interactions: Relevance to adhesion and adhesive bonding. *Handbook of Adhesive Technology* **2003**, 95-144.
36. Akbey, Ü .; Graf, R.; Peng, Y. G.; Chu, P. P.; Spiess, H. W., Solid-State NMR investigations of anhydrous proton-conducting acid–base poly(acrylic acid)– poly(4-vinyl pyridine) polymer blend

system: A study of hydrogen bonding and proton conduction. *Journal of Polymer Science Part B: Polymer Physics* **2009,** *47* (2), 138-155.
37. Lee, J. H.; Lee, D. W., Contact-induced molecular rearrangement of acrylic acid-incorporated pressure sensitive adhesives. *Applied Surface Science* **2020,** *500*, 144246.
38. Polymer Properties Database, Stress relaxation processes, Access date: July 18, 2019, DOI: http://polymerdatabase.com/polymer%20physics/Relaxation.html.
39. Bower, D. I., Morphology and motion. In *An Introduction to Polymer Physics*, Cambridge University Press: Cambridge, 2002; pp 117-161.
40. MacKenzie, C. I.; Scanlan, J., Stress relaxation in carbon-black-filled rubber vulcanizates at moderate strains. *Polymer* **1984,** *25* (4), 559-568.
41. Mitra, S.; Chattopadhyay, S.; Bhowmick, A. K., Dynamic stress relaxation behavior of nanogel filled elastomers. *Journal of Polymer Research* **2011,** *18* (4), 489-497.
42. Doi, M.; Edwards, S. F., In *The Theory of Polymer Dynamics*, Oxford University Press: Oxford, 1986.
43. Rinde, J. A., Poisson's ratio for rigid plastic foams. *Journal of Applied Polymer Science* **1970,** *14* (8), 1913-1926.
44. Sierros, K. A.; Morris, N. J.; Ramji, K.; Cairns, D. R., Stress–corrosion cracking of indium tin oxide coated polyethylene terephthalate for flexible optoelectronic devices. *Thin Solid Films* **2009,** *517* (8), 2590-2595.
45. Everaerts, A. I.; Xia, J., *Adhesives compatible with corrosion sensitive layers*. United States Patents: 2010; Vol. US 2010/0040842A1 ; 2010.
46. Leung, W. S.; Chan, Y. C.; Lui, S. M., A study of degradation of indium tin oxide thin films on glass for display applications. *Microelectronic Engineering* **2013,** *101*, 1-7.

Acknowledgements

I have been dreaming of being a professor and a president of the university at which inspired me to have personal and professional goals since I was an undergraduate student. These pronounced goals have facilitated me to go on and on, and stood me upright whenever I faced mountains and valleys during Master's study. At first, I was fretful, blaming the points which were unsatisfactory and I cannot be compatible with. Yet, once I realized that this is the part of getting through and reflected the story of Isaac and Beer-sheba (Genesis 26:1-33), I just thank the Lord, God for all he has done to me. I am satisfied if my colleagues see and know the Lord, God through me although some may try to take advantage of me. After this realization, I saw how he has worked through me, and my performance during M.S. has substantiated my sayings (just in my personal point of view); I well-understood how I am myself. I felt that every atmosphere was designed to train me. I believe that pursuing M.S. at UNIST was the valuable first step heading toward the goals in terms of personal and academic improvement. I thank my advisor Prof. D. W. Lee for his belief that he allowed me to explore my research interest within the scope of filler-reinforced pressure sensitive adhesives without project-oriented constraints. I hope that prospective/current M.S. or Ph. D. candidates in our research group will surpass my outcomes, producing exceptional performance, which implies improvement and development of science and technology in our country. Finally, I appreciate my parents who brought me up as a Christian. I love you.